PEOPLE'S DEMOCRATIC REPUBLIC OF ALGERIA

MINISTRY OF HIGH EDUCATION AND SCIENTIFIC RESEARCH

UNIVERSITY YAHIA FARES OF MEDEA

Faculty of Technology

DEPARTMENT of PROCESS ENGINEERING AND ENVIRONMENT

MASTER THESIS

Branch: Process Engineering

Major: Chemical Engineering

Theme:

Modeling Pressure Drop in Fluidized Cylindrical and Conical Beds

Presented by:

HANANI Islam Samer Hafthe

Proposed and Directed by:

LAIDI Maamar

HANINI Salah

Academic Year 2023 / 2024

I dedicate this work to those who gave me everything, to those who have always been a source of inspiration for me in times of distress, to those who have reached where I am just so they can be proud of me, my beloved family, to the source of eternal giving and love, my dear mother, to my first and last support in this world, may God keep him alive my beloved father, to my brothers, Hamza, Ahmed, Abdul Rahman, and my wonderful family.

I dedicate this work to my beloved homeland, Palestine, and to all its martyrs, wounded, and prisoners.

To the great Algeria that embraced us for five years and made us engineers, and to its good people, especially my dear friend, to whom the days made us brothers Abdul Malek, and to his very good mother, Siham, and his good father, Omar.

To **Dr. Madani Achouak**, who always provided assistance until this work saw the light.

To all my international friends who have been together in Algeria for five years.

To everyone who was supportive of me throughout my school years.

To all my acquaintances and my extended family.

First of all, we praise and thank God Almighty from the bottom of our hearts for His generous gift to us by making us among His servants as scholars and by granting us to see the day in which our academic efforts will be crowned with graduation.

I would like to extend my sincere thanks from my heart to the supervisor, **Professor Laidi Maamar**, and the supervisor, the great **Professor Hanini Salah**, for all their time, their efforts, and their good treatment of me throughout this period, as they were always present in times of need and made every possible effort so that this work could see the light.

To the doctor who had a great influence and who helped me from the beginning of completing this work until the last day of it, who always helped me with work and information, and who was always present in difficult times, **Dr. Madani Achouak.**

To myself, who endured all the hardships, worked hard, and never gave up.

Finally, to everyone who had an impact on the completion of this work, directly or indirectly, including all the doctors and professors in the Department of Process Engineering and Environmental in Yahya Fares University.

ملخص: نمذجة انخفاض الضغط في السرير المميع الاسطواني والمخروطي

تقدم هذه الدراسة منهجية جديدة مبتكرة لنمذجة انخفاض الضغط في الطبقات المميعة الاسطوانية والمخروطية باستخدام اربع خوارزميات مختلفة, آلة ناقل الدعم (SVM), وايضا (SVM) بالتزامن مع ثلاث خوارزميات تحسين فوقية وهي: تحسين سرب الجسيمات (PSO), خوارزمية اليعسوب (DA), ومحسن الذئب الرمادي (GWO), وعلى النقيض من الطرق التقليدية تستعمل طريقتنا معلمات بدون ابعاد مثل رقم رينولدز في عملية النمذجة. يمثل عملنا اسهام فريد في عالم فقدان الضغط في السرير المميع حيث لم يسبق أن تم التنبؤ بفقدان الضغط باستعمال الة ناقل الدعم (SVM), وايضا يمثل استعمال المعلمات بدون ابعاد خروج عن الممارسات التقليدية في هذا المجال. من خلال التقييم الشامل حقق نموذجنا الافضل بدون ابعاد وباستعمال SVM-PSO اداء معامل تحديد (R^2) مبهر يبلغ 997.0 وخطأ مربع لمتوسط الجذر(RMSE) منخفض قدره 0.047 ومتوسط انحراف نسبي مطلق (AARD) يساوي 0.5235%, متجاوزا وبقوة اداء المعلمات التقليدية. يؤدي استخدام الأرقام بدون أبعاد إلى تسهيل إمكانية المقارنة والتعميم بشكل أفضل عبر إعدادات وظروف تجريبية مختلفة، كما يتيح وضع نماذج أكثر قوة ودقة عن طريق تقليل تأثير اختلافات المقياس المتأصلة في البيانات الأولية. يوضح هذا الاكتشاف المهم إمكانية الاستفادة من الأرقام التي لا أبعاد لها للتنبؤ الدقيق بانخفاض الضغط في الطبقات المميعة ويقترح طرقًا واعدة لمزيد من البحث في هذا المجال.

الكلمات المفتاحية: انخفاض الضغط, السرير المميع, تمييع, آلة ناقل الدعم, خوارزمية اليعسوب, تحسين سرب الجسيمات, محسن الذئب الرمادي.

Abstract: Modeling Pressure Drop in Fluidized Cylindrical and Conical Beds

This study introduces an innovative methodology for modeling pressure drop in cylindrical and conical fluidized beds, employing four different algorithms, Support Vector Machine (SVM), and (SVM) in conjunction with three optimization algorithms: Particle Swarm Optimization (PSO), Dragonfly Algorithm (DA), and Grey Wolf Optimizer (GWO). Unlike conventional approaches, our method integrates dimensionless parameters, such as the Reynolds number, into the modeling process. This novel inclusion of dimensionless numbers represents a departure from traditional practices in the field. Through comprehensive evaluation, our best-performing dimensionless model using SVM-PSO achieved an impressive coefficient of determination (R^2) of 0.99715, a Root Mean Square Error (RMSE) of 0.047, and an average absolute relative deviation (AARD) of 0.5235% when trained on the dimensionless parameters dataset, exceeding the performance of the traditional parameters. Utilizing dimensionless numbers facilitates better comparability and generalizability across different experimental setups and conditions, and it enables more robust and accurate modeling by reducing the influence of scale variations inherent in raw data. This significant finding demonstrates the potential of leveraging dimensionless numbers for accurate prediction of pressure drop in fluidized beds and suggests promising avenues for further research in this domain.

KEYWORDS: Pressure drop, fluidized bed, fluidization, support vector machine, dragonfly algorithm, particle swarm optimization, grey wolf optimizer.

Résumé : Modélisation de la perte de charge dans les lits fluidisés cylindriques et coniques

Cette étude présente une méthodologie innovante pour modéliser la chute de pression dans les lits fluidisés cylindriques et coniques, utilisant quatre algorithmes différents (SVM), (SVM) en conjonction avec trois algorithmes d'optimisation hybrides: Partiale Swarm Optimization (PSO), Dragonfly Algorithme (DA), Grey Wolf Optimizer (GWO), et pour notre méthode intégré des paramètres sans dimension tel que le nombre de Reynolds, cette nouvelle inclusion représente une rupture avec les pratiques traditionnelles dans le domaine, notre modèle a atteint une coefficient de détermination(R^2) impressionnât de 0.99715, erreur quadratique moyenne RMSE de 0.047, et (AARD) de 0.5235%, l'utilisation de cette méthode facilite une meilleure comparabilité, généralisable dans différents configurations, et permet une modélisation plus robuste et précise en réduisant l'influence des variations, cette découverte importante pour une prévision précise de la chute pression dans les lits fluidisés, et suggère des pistes pous plus des recherches.

MOTS CLÉS: Perte de charge, lit fluidisé, fluidisation, machine à vecteurs de support, algorithme de libellule, optimisation des essaims de particules, optimiseur de loup gris..

General Introduction ..... - 1 -

Chapter I: Generalize about pressure drop in fluidization

I.1. Introduction ..... - 4 -

I.2. Fundamentals of fluidization ..... - 4 -

I.2.1. Definition of fluidization ..... - 4 -

I.2.2. Types of fluidization ..... - 4 -

I.2.3. Advantages and disadvantages of fluidization ..... - 5 -

I.2.3.1. Advantages of fluidization ..... - 5 -

I.2.3.2. Disadvantages of fluidization ..... - 5 -

I.3. Fundamentals of pressure drop in fluidization ..... - 6 -

I.3.1. Historical review ..... - 6 -

I.3.2. Definition of pressure drop in fluidized beds ..... - 7 -

I.3.3. Effects of operating parameters on pressure drop ..... - 8 -

I.3.3.1. Fluidization velocity ..... - 8 -

I.3.3.2. Column diameter and bed height ..... - 9 -

I.3.3.3. Porosity ..... - 9 -

I.3.3.4. Diameter and density of particle ..... - 10 -

I.3.3.5. Viscosity of fluid ..... - 11 -

I.3.3.6. Density of Fluid ..... - 11 -

I.3.3.7. Bed Geometry ..... - 11 -

I.3.3.7.1. Cylindrical beds ..... - 11 -

I.3.3.7.2. Conical beds ..... - 12 -

I.3.4. Mechanisms contributing to pressure drop ..... - 13 -

I.3.4.1. Frictional losses ..... - 13 -

I.3.4.2. Acceleration losses ..... - 14 -

I.3.4.3. Expansion losses ..... - 14 -

I.4. Experimental Techniques for Pressure Drop Measurement ..... - 14 -

I.4.1. Overview of experimental methods for measuring pressure drop in fluidized beds ..... - 14 -

I.4.1.1. Pressure sensors ..... - 14 -

I.4.1.2. Manometers ..... - 15 -

I.4.1.3. Pitot tubes ..... - 16 -

I.4.2. Considerations for experimental setup and data acquisition ..... - 16 -

I.4.3. Case studies highlighting experimental investigations of pressure drop in fluidized systems - 17 -

I.5. Pressure drop models - 17 -

I.5.1. Forchheimer correlation - 18 -

I.5.2. Blake–Kozeny equation - 19 -

I.5.3. Burke–Plummer equation - 19 -

I.5.4. Ergun equation - 20 -

I.6. Application of pressure drop analysis in industrial processes - 21 -

I.7. Conclusion - 21 -

Chapter II: Generalize about artificial intelligence

II.1. Introduction - 22 -

II.2. Historical Review - 22 -

II.3. Definition of Artificial Intelligence - 24 -

II.4. The main classification of AI - 24 -

II.4.1. Weak artificial intelligence - 25 -

II.4.2. Powerful artificial intelligence - 25 -

II.5. Types of Artificial Intelligence - 25 -

II.5.1. Machine learning - 25 -

II.5.2. Natural language processing - 26 -

II.5.3. Speech - 26 -

II.5.4. Planning - 26 -

II.6. AI algorithm - 27 -

II.6.1. Definition of AI algorithm - 27 -

II.6.2. AI algorithms work - 27 -

II.6.3. Types of Artificial Intelligence Algorithms - 28 -

II.6.3.1. Reinforcement learning - 28 -

II.6.3.2. Unsupervised learning - 28 -

II.6.3.3. Supervised learning - 28 -

II.6.3.3.1. Decision Tree - 29 -

II.6.3.3.2. Support Vector Machines - 29 -

II.6.4. Meta-heuristic algorithms - 32 -

II.6.4.1. Particle swarm optimization - 32 -

II.6.4.2. Dragonfly algorithm - 34 -

II.6.4.3. Grey wolf optimizer - 36 -

II.7. Conclusion ..... - 38 -

Chapter III: Experimental Study and Modeling of Pressure Drop in Fluidized Beds

III.I. Introduction ..... - 39 -

III.2. Methodology ..... - 39 -

III.2.1. Data-set collection and pretreatment ..... - 39 -

III.2.1.1. Normal model ..... - 39 -

III.2.1.2. Dimensionless model ..... - 40 -

III.2.2. Data division and model development ..... - 41 -

III.3. Results and Discussion ..... - 42 -

III.3.1. Effect of inputs on output ..... - 42 -

III.3.1.1. Relative importance of inputs ..... - 42 -

III.3.1.2. Violin boxplot of the effect of inputs ..... - 44 -

III.3.2. SVR models development ..... - 45 -

III.3.2.1. Support vector regression model ..... - 45 -

III.3.2.2. SVR-dragonfly algorithm model ..... - 47 -

III.3.2.3. SVR- grey wolf optimizer model ..... - 49 -

III.3.2.4. SVR- particle swarm optimization model ..... - 51 -

III.3.2.6. General comparisons ..... - 54 -

III.4. Conclusion ..... - 60 -

General Conclusion ..... - 61 -

Chapter I: Generalize about pressure drop in fluidization

Figure I. 1. The different types of fluidization **[27]** ..... - 5 -
Figure I. 2. Different bed conditions with increased with a difference pressure drop **[35]** ..... - 8 -
Figure I. 3. Relationship curve between pressure drop and fluidization velocity **[38]** ..... - 9 -
Figure I. 4. Pores in a porous medium **[41]** ..... - 10 -
Figure I. 5. Example of cylindrical beds **[47]** ..... - 12 -
Figure I. 6. Example of conical beds **[49]** ..... - 13 -
Figure I. 7. Layout reviews installing pressure sensors on the bed **[55]** ..... - 15 -

Chapter II: Generalize about artificial intelligence

Figure II. 1. The parts of the brain responsible for hunger **[71]** ..... - 23 -
Figure II. 2. The main classification of AI **[74]** ..... - 25 -
Figure II. 3. Types of artificial intelligence **[78]** ..... - 27 -
Figure II. 4. The form general of SVR **[88]** ..... - 32 -
Figure II. 5. The conceptual framework for identifying the best visit point in a swarm **[95]** ..... - 33 -
Figure II. 6. Simple correction patterns amongst members of a swarm **[96]** ..... - 36 -

Chapter III: Experimental Study and Modeling of Pressure Drop in Fluidized Beds

Figure III. 1. Histogram of inputs' relative importance (Normal model) ..... - 43 -
Figure III. 2. Histogram of inputs' relative importance (Dimensionless model) ..... - 43 -
Figure III. 3. Violin plots of the effect of inputs on output (Normal model) ..... - 44 -
Figure III. 4. Violin plots of the effect of inputs on output (Dimensionless model) ..... - 45 -
Figure III. 5. Actual versus the predicted pressure drop values by the SVR model ..... - 46 -
Figure III. 6. Actual versus the predicted Euler number values by the SVR model ..... - 47 -
Figure III. 7. Actual versus the predicted pressure drop values by the SVR-DA model ..... - 48 -
Figure III. 8. Actual versus the predicted Euler number values by the SVR-DA model ..... - 49 -
Figure III. 9. Actual versus the predicted pressure drop values by the SVR-GWO ..... - 50 -
Figure III. 10. Actual versus the predicted Euler number values by the SVR-GWO ..... - 51 -
Figure III. 11. Actual versus the predicted pressure drop values by the SVR-PSO model ..... - 52 -
Figure III. 12. Actual versus the predicted Euler number values by the SVR-PSO ..... - 53 -
Figure III. 13. Kernel density estimation plot for SVR model ..... - 56 -
Figure III. 14. Kernel density estimation plot for SVR-GWO model ..... - 56 -
Figure III. 15. Kernel density estimation plot for SVR-DA model ..... - 57 -
Figure III. 16. Kernel density estimation plot for SVR-PSO model ..... - 57 -
Figure III. 17. Correlation plot between inputs (Normal model) ..... - 58 -
Figure III. 18. Correlation plot between inputs (Dimensionless model) ..... - 58 -
Figure III. 19. Chart column of R2 and RMSE for all models ..... - 59 -
Figure III. 20. 3D pie for the number of Average absolute relative deviation (AARD) for different ranges ..... - 59 -

Chapter I: Generalize about pressure drop in fluidization

Table I. 1. Several experimental tests for pressure drop in fluidization, with most prominent results. .- 17 -

Chapter III: Experimental Study and Modeling of Pressure Drop in Fluidized Beds

Table III. 1. Data ranges (Normal model) .....- 41 -
Table III. 2. Data ranges (Dimensionless model).....- 41 -
Table III. 3. External validation criteria for all models .....- 54 -

AI: Artificial Intelligence

ANN: Artificial Neural Network

CCC: Concordance Correlation Coefficient

CPU: Central Processing Unit

DA: Dragonfly Algorithm

GWO: Grey Wolf Optimizer

HCI: Human-Computer Interface

PSO: Particle Swarm Optimization

QP: Quadratic Programming

RBF: Radial Basis Function

SVR: Support Vector Regression

General Introduction

General Introduction

The fluidization process and in particular, the pressure drop (ΔP) in it is considered one of the processes that require precise adjustment of many parameters to obtain good results. Therefore, it is considered difficult to build accurate dynamics to control it. Many existing models have been developed based on mass and energy conservation equations to develop these models **[1]**, but this was not feasible from a standpoint technical and economic **[2]**, and from here we turned to artificial intelligence techniques such as artificial neural networks (ANNs) and support vector machines (SVMs)Which are considered effective methods in this field **[3-5]**.

One of the challenges faced by students, teachers, and even experienced engineers in various fields of study and research, especially in the field of chemical engineering, is the use of different measurement systems. Although there is an international system of units (SI) that is widely used in mathematical equations, many places and countries still use alternative systems. Moreover, some experimental correlations for physical and chemical properties used in various equipment cannot be easily obtained in the international system. This can make it difficult for professionals to communicate and collaborate effectively and may lead to errors in calculations and measurements, **[6]** another problem is some international standards do not cover chemical engineering quantities and units **[7].** It is possible to make errors when deriving units in derived units, certain publishing houses don't mandate writers to use a particular system of measurement **[8].**

Fluidized beds are typically employed when is required a high contact area between solid particles and a fluid phase **[9]**, fluidized beds are usually constructed in two main shapes: cylindrical and conical, and we cannot ignore the fact that the cylindrical shape is the most widely known **[10]**, it is used in chemical engineering operations for processes like absorption, distillation, adsorption, and catalysis **[11]**, reactor systems and heat transfer **[12]**, however, in some fields, the need for conical fluidized beds appears because they have some properties that are not found in a cylindrical bed, such as the gradation in the sizes of particles in the bed. Among these industries is the pharmaceutical industry **[13]**.

One of the main obstacles facing anyone who wants to use machine learning techniques is the number of parameters that must be adjusted accurately and correctly, whether the adjustment is manual or through trial and error, to ensure that the algorithm runs correctly **[14]**, especially in the

field of chemical engineering, in which artificial intelligence is usually not used, despite the large number of applications in which it can be employed in this field **[15]**, especially using the support vector machine (SVM), which has gained great popularity due to many features such as the possibility of non-linear modeling of processes, and the dimensions of the input space do not matter when used **[16]**. We remain faced with the problem of determining the optimal parameters to achieve the best result **[17].** Therefore, a meta-heuristic optimization algorithm was used to find and adjust the best parameters within a short time **[18],** many meta-heuristic optimization algorithms have been modeled whose structure is inferred from nature **[19],** in this work, we used Particle Swarm Optimization (PSO), which has the advantages of ease of use, requires only a small number of parameters, and is effective in the field of computing. It has proven its reliability well **[20],** Grey Wolf Optimizer (GWO) was also used, which proved to be very good in premature convergence and local optimization problems **[21],** Finally, we used Dragonfly Algorithm (DA), which is the latest among all of the above, and whose advantages include accelerated operations to obtain effective solutions, and suitability for various optimization problems **[22].** We have used the previous skillful optimization algorithms in addition to the algorithm of (SVM) to calculate pressure drop prediction in fluidized beds to come up with several results for comparison.

There is no literature exists concerning the utilization of Support Vector Machine (SVM) algorithms for predicting pressure drop (ΔP) within cylindrical and conical beds in the context of fluidization. Moreover, there is a discernible lack of inclination toward the adoption of SVM methodologies within the discipline of fluidization research.

Therefore, this work aims to build four models Support vector machine(SVM), SVM-Particle Swarm Optimization (PSO), SVM-Dragonfly Algorithm(DA), and SVM-Gray Wolf Optimizer (GWO) to predict pressure drop (ΔP) and compare the four different results with each other, and to compare the two models, the normal one and the dimensionless model, and to draw the results of the final study to be the first in this field.

For this purpose, we divide our work into 03 chapters

Chapter I: Generalize about pressure drop in fluidization, this chapter is dedicated to giving a general idea about pressure drop in fluidization and discusses its basic matters.

Chapter II: Generalize about artificial intelligence, in this chapter, we talk about Artificial Intelligence, which defines it and gives us a look at it, we also talk about the algorithms that we will use in our work and their basic structure.

Chapter III: Experimental Study and Modeling of Pressure Drop in Fluidized Beds, the third chapter in which we will talk about the detailed steps for modeling our work, from preparing databases to the methods and metrics used, then reviewing the results of different models, leading to the comparison between them in more than one aspect and in more than one way.

Finally, in conclusion, we will recall the essential results obtained and we will propose perspectives of our study.

Chapter I: Generalize about pressure drop in fluidization

I.1. Introduction

The first appearance of fluidized bed processes in industrial circles occurred in 1920s **[12]** when it emerged and emerged academically as a new field of chemical engineering sciences and a phenomenon of transportation, especially in the fifties of the last century. Its development continued over the years until it became today one of the fields that have made a great difference and achievements, especially in operations like converting coal, petroleum, and water refining into the food, agricultural, and pharmaceutical fields **[23]**.

Perhaps one of the most important factors that must be understood in the fluidization process to obtain good operational efficiency is the pressure drop, as an excessive decrease in it means increased costs, equipment wear, and other things that we will learn about below **[24].**

In this chapter, we will talk about the fluidization process in general, define it, and mention its basic types. In addition, we will move to pressure drop and explain its characteristics and the most important factors affecting it.

I.2. Fundamentals of fluidization

I.2.1. Definition of fluidization

The process of fluidization is defined as making a solid substance behave like a liquid by passing a gas or liquid upward through it. One of the most important features of this process is the high ability to transfer heat and mass between the fluid and solid phases, so it is widely used in various physical and chemical processes **[25,26].**

I.2.2. Types of fluidization

Depending on the type of material being fluidized, there are five distinct types of fluidization that can occur. These are, homogeneous, bubbling, sluggish, turbulent, and spouting, as described by Kunii and Levenspiel 1991 **[27].**

In the following Figure I.1 we review the different types of the fluidization process.

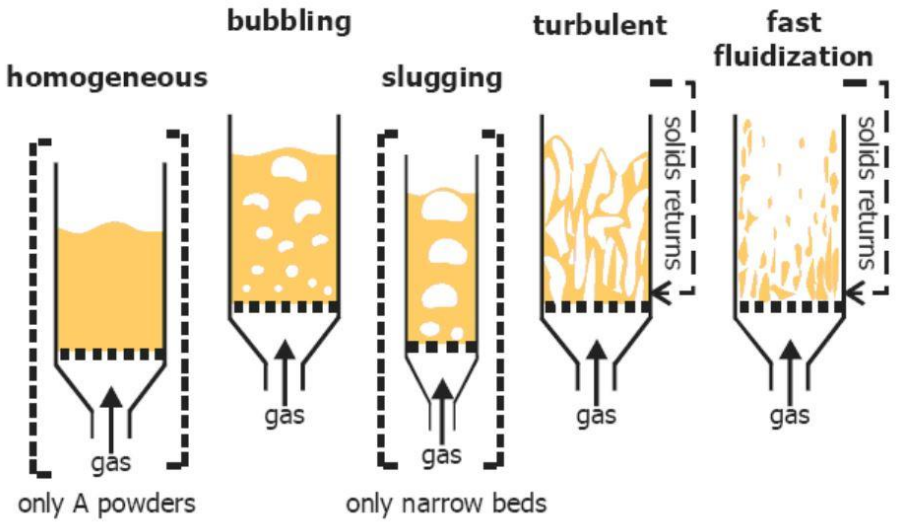


Figure I. 1. The different types of fluidization **[27]**

I.2.3. Advantages and disadvantages of fluidization

I.2.3.1. Advantages of fluidization

There are many different and diverse benefits to the fluidization process, including **[28]**:

- Superior Heat Transfer: Fluidized beds are perfect for processes like drying, roasting, and calcination that call for high heat transfer rates because of their superior heat transfer qualities;
- Uniform mixing: Fluidization guarantees even dispersion of solid particles, leading to a more stable end product quality;
- Continuous operation: Because fluidized beds may run continuously, throughput can be increased and process control can be improved;
- Low-pressure drop: Low-pressure drops allow fluidized beds to function, which lowers energy use and operational expenses.

I.2.3.2. Disadvantages of fluidization

In addition to the advantages, the fluidization process, like other processes, has disadvantages, including **[29]:**

- Uneven contact between gas and solid: The primary disadvantage of gas-solid fluidizationis the unequal contact between steel and gas, which leads to insufficient reactions in some cases;
- Corrosion of internal bed parts: The rapid velocity of the liquid can corrode the internal parts of the bed, resulting in shortened equipment life and higher maintenance costs;
- Depletion of solids: The fluidization process has the ability to reduce the size of solid particles and produce finer particles;
- Possibility of entrapment of solid particles with liquid: Entrapment of solid particles with liquid can cause contamination of downstream equipment, reducing efficiency and increasing maintenance costs;
- Complexity of design and operation: The design and operation of fluidized beds can be complex, requiring specific knowledge and experience.

I.3. Fundamentals of pressure drop in fluidization

I.3.1. Historical review

Since fluidization became available at the beginning of the twentieth century and the beginning of the popularity of its various applications, this aspect has received the attention of many scientists to conduct their studies on it. Perhaps one of the most prominent research that appeared, in the beginning, was the pioneering works of Fritz Winkler, since the phenomenon of fluidization began to spread in the 1930s, scientists have increased their interest in it **[30]**, leading up to Winkler's research in the 1940s, which was concerned with exploring the hydrodynamics of fluidized beds, including the characteristics of pressure drop **[31]**. These early studies established basic insights into the fluidization process, but they lacked equipment. Good computational tools are available today.

After that, a major leap occurred in the world of fluidization, thanks to scientists such as Octave Levenspiel and Warren K. Lewis. Levenspiel developed experimental relationships to predict pressure drops in fluidized beds **[32]**, while Lewis and his colleagues made a difference by formulating various mathematical models to describe fluid dynamics and phenomena. Related to heat transfer in fluidized systems **[33]**, these theoretical developments contributed significantly to a greater understanding of pressure drop and subsequently facilitated the design of fluidized bed reactors and other industrial equipment.

The theoretical side of the mathematical models continued to be developed until experimental studies were considered important to verify the validity of the theoretical models and to develop experimental correlations. Many experiments were conducted by researchers to verify the characteristics of the pressure drop under different operating conditions such as different bed heights, gas flow rates, and particle sizes. Perhaps one of the most prominent of these studies is the study by Davidson and Harrison in the 1970s, in which they used advanced instrumentation techniques to measure the pressure drop in fluidized layers **[34]**. The results they reached were considered highly valuable data for validating theoretical predictions and increasing the accuracy of experimental correlations.

In summary of all that was said previously, the study of pressure drop in fluidization has witnessed great development over the past century thanks to the efforts of researchers from various disciplines. This field witnessed a qualitative leap from early experimental investigations to the development of advanced theoretical models, and reaching a much deeper understanding of fluidization, which contributed to its arrival on a wide scale. From industries, and as researchers continue to develop theoretical models and improve various measurement tools, the last step in developing this field is to introduce it into the world of artificial intelligence to obtain predictive models based on machine learning algorithms.

I.3.2. Definition of pressure drop in fluidized beds

The pressure drop in fluidization refers to the decrease in pressure between two points in the system when the fluid passes through it because when the fluid passes through the particles, it applies an upward pulling force to them. It is a crucial parameter in fluidized bed systems because it has a major role in the behavior of the layer and the efficiency of the system which is a phenomenon that must be studied to understand the fluid dynamics within the layer and improve processes. Yes, it can be expressed in another language as the decrease in pressure that results from the movement of the gas through a layer of molecules **[12].**

In the following Figure I.2, we review the different bed conditions with a difference pressure drop.

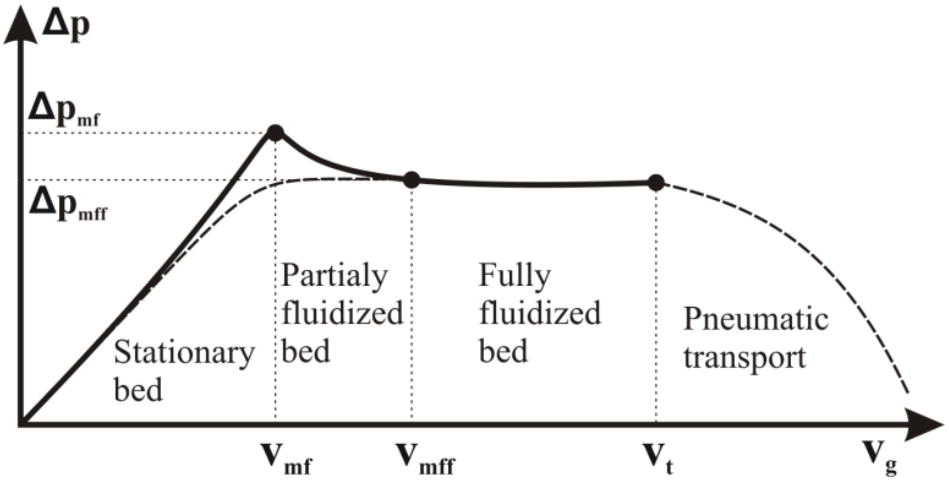


Figure I. 2. Different bed conditions with increased with a difference pressure drop **[35]**

I.3.3. Effects of operating parameters on pressure drop

There are many parameters that affect, in varying proportions, the pressure drop in the fluidized bed, whether these parameters are specific to the fluid used or the bed in which fluidization occurred. The most important of these parameters are:

I.3.3.1. Fluidization velocity

The fluidization velocity is one of the most important parameters that is considered when talking about the pressure drop in the fluidization process. The major role it plays is that the greater the fluidization velocity the greater the pressure drop until a certain point is reached, called the minimum fluidization velocity (U_{mf}), which is the point that separates the fixed bed from the fluidized bed, where after reaching this point the pressure drop almost stabilizes even with increasing velocity and is accompanied by an increase in the height of the fluidized bed with the possibility of bubbles appearing, as the Figure I.3 which shows the relationship curve between pressure drop and fluidization velocity **[36,37]**:

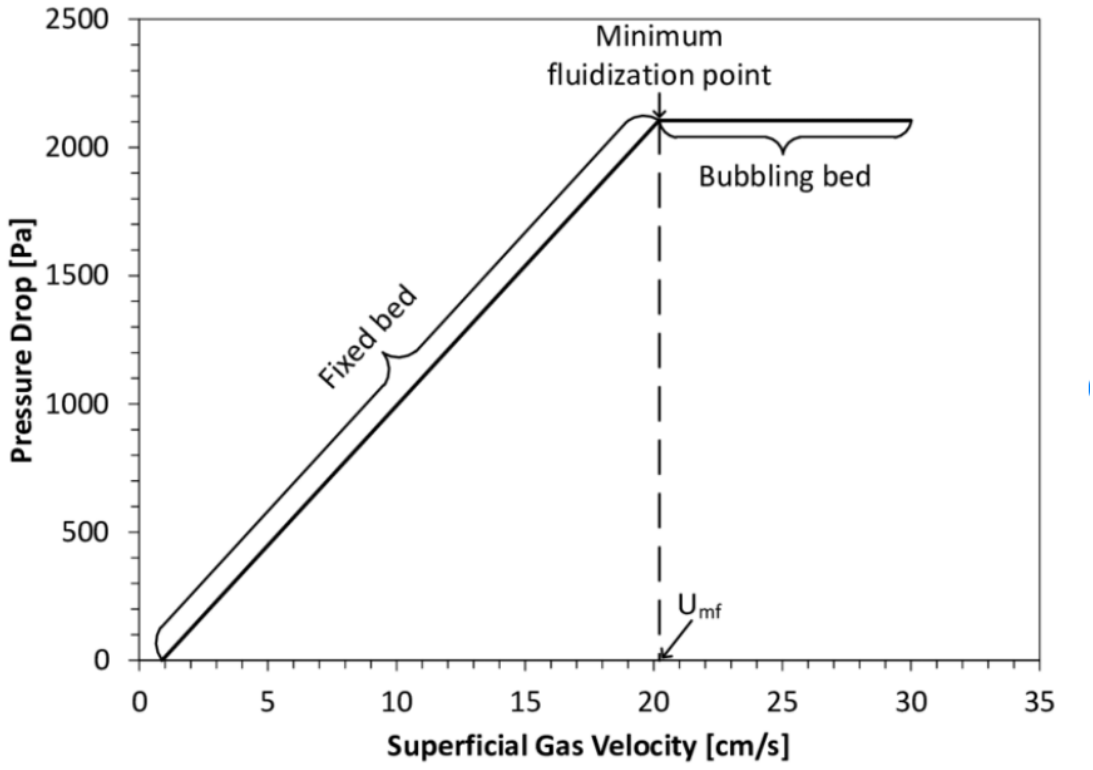


Figure I. 3. Relationship curve between pressure drop and fluidization velocity **[38]**

I.3.3.2. Column diameter and bed height

Many studies have been concerned with studying the effect of column diameter and bed height on pressure drop. It has been proven through experiments that reducing the column diameter leads to an increase in the minimum fluidization velocity, which leads to an increase in pressure drop in fluidized bed systems. Increasing the bed height leads to an increase in The pressure drop in the fluidized layer, which confirms its effect on pressure drop **[39]**.

I.3.3.3. Porosity

Porosity is the percentage of void volume in the bed and plays an important role in the fluidization process. It is one of the parameters that attracted many researchers to study it and its effect on the fluidization process in general and pressure drop in particular. As for the effect it plays on pressure drop, with increasing porosity The pressure drop in the bed decreases. This fact is because as the layer expands and the porosity rises, the total drag on the particles decreases **[40]**. It is calculated through the following relationship:

$$\varepsilon = \frac{(Vt - Vs)}{V_t} \qquad (I.1)$$

Where V_t is the volume total or volume of the bed and V_s is the volume of solids or particles. The following Figure I.4 shows an example of pores between solid molecules in a porous medium.

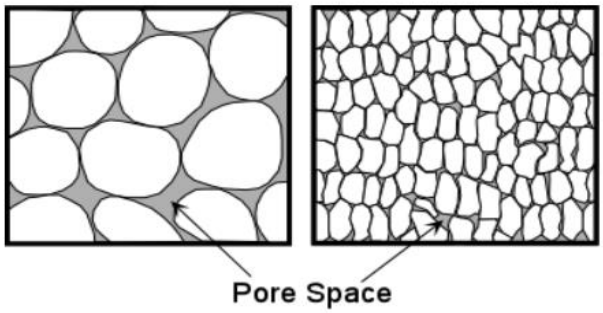


Figure I. 4. Pores in a porous medium **[41]**

I.3.3.4. Diameter and density of particle

The effect that particle diameter plays on pressure drop is a complex phenomenon that involves many different factors, as some studies indicated a significant decrease in the minimum fluidization velocity with the addition of smaller particles, and other studies showed an increase in pressure drop with a decrease in particle diameter, as a summary of the above art. Much research indicates that while smaller particles can reduce the minimum fluidization velocity, they may also increase the pressure drop, and other factors such as particle shape can further complicate the relationship. We also cannot ignore the particle density and its effect on the pressure drop, since as the particle density increases, the fluidized bed becomes more stable, which leads to a decrease in vacuum, meaning that the greater the particle density, the greater the pressure drop **[42-45]**. The particle density can be calculated from the relationship:

$$\rho_s = \frac{m_s}{V_s} \qquad (I.2)$$

where is m_s the mass of particles and V_s is the volume of particles.

I.3.3.5. Viscosity of fluid

Increasing the viscosity of the fluid leads to an increase in the minimum fluidization velocity. The reason for this increase is that the more viscosity the fluid increases, the more force it requires to move the solid particles, which leads to a greater increase in pressure drop across the layer. In addition, turbulence within the vicinity of the fluidized bed can be reduced, leading to lower pressure across the fluidized bed. There are other factors related to viscosity, such as temperature and geometry of the fluidized bed, which are factors that must be carefully considered when designing a class system **[46]**.

I.3.3.6. Density of Fluid

An increase in fluid density leads to an increase in pressure drop in the fluidized bed. This relationship is affected by other factors such as particle size, particle density, and fluid velocity. It is very important to focus on fluid density and its relationship to pressure drop to reach a deeper understanding of how fluid properties affect the dynamics of the fluidization process in general **[12]**. The fluid density can be calculated from the relationship:

$$\rho_f = \frac{m_f}{V_f} \qquad \text{(I.3)}$$

Where m_f is the mass of fluids and V_f is the volume of fluids.

I.3.3.7. Bed Geometry

The bed geometry is one of the pivotal parameters in the process of fluidization and pressure drop as we mentioned previously, things such as the height of the bed and the diameter of the pipe play important roles. There is an aspect that we did not talk about that also plays an important role, which is the shape of the bed. It can be divided into the two most famous forms:

I.3.3.7.1. Cylindrical beds

Cylindrical beds, also known as packed beds, are commonly used in chemical engineering processes that require rapid transfer of mass and heat, such as catalytic chemical reactions, and the ability to move and mix molecules easily within the bed. The pressure is calculated using the Ergun equation, and pressure drop is one of the things that is taken into consideration when designing and operating these systems. Below is a Figure I.5 showing the general appearance of this family **[11]**:

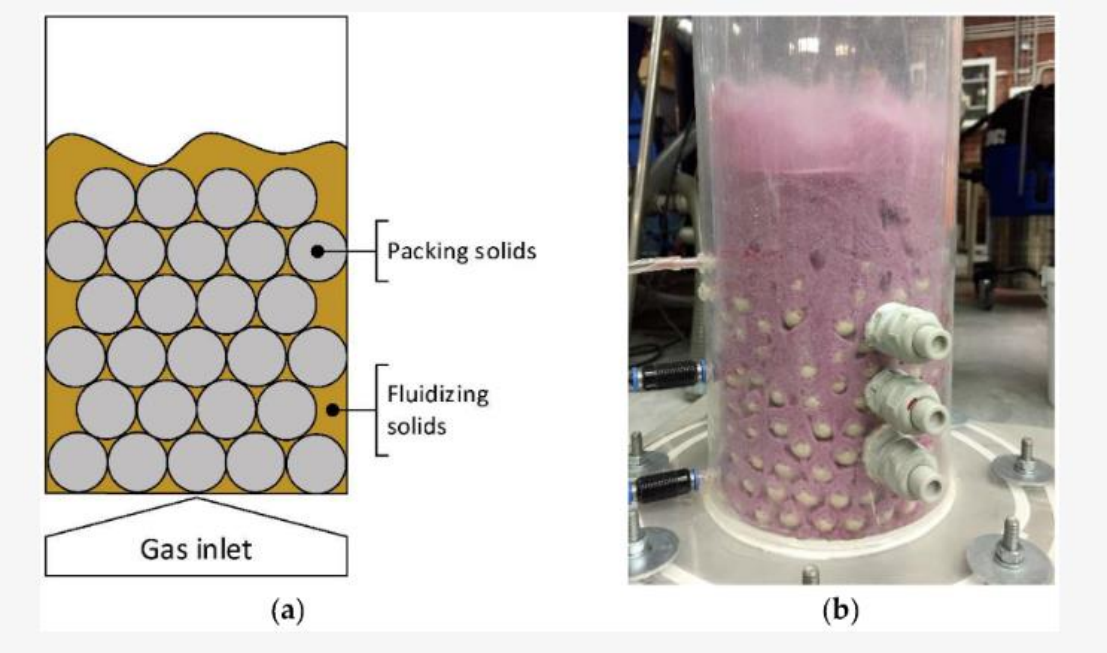


Figure I. 5. Example of cylindrical beds **[47]**

I.3.3.7.2. Conical beds

The geometric effect of the conical bed has a significant impact on pressure drop, as after conducting experiments it was found that it is useful in the process of reducing pressure and therefore very useful in reducing costs in fluidization operations. The following Figure I.6 shows the general appearance of this type of bed **[48]:**

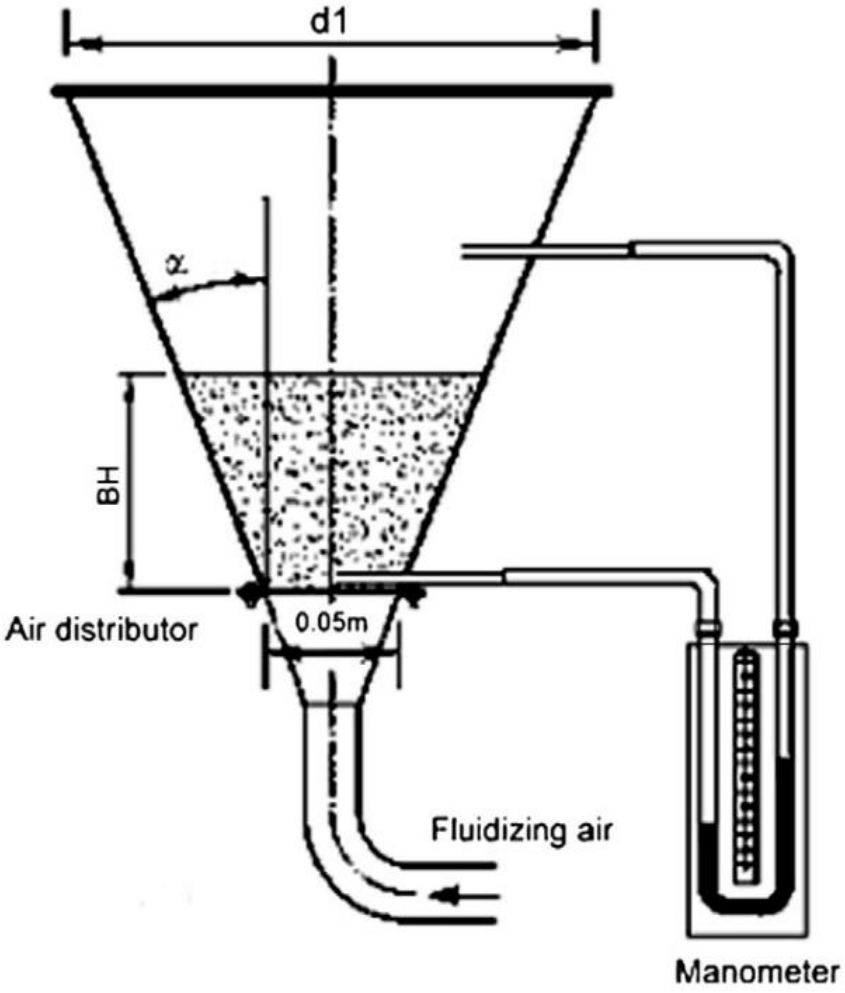


Figure I. 6. Example of conical beds **[49]**

I.3.4. Mechanisms contributing to pressure drop

Many other factors affect the pressure drop processand are taken into account when we talk aboutthe fluidization process, the most important of which are:

I.3.4.1. Frictional losses

Friction losses are an important factor in fluidization systems that lead to pressure drop. Friction loss is defined as the energy lost in the fluidization process due to friction between the fluid and the pipe walls. From the previous definition, we conclude that the loss of friction is proportional to the length of the pipe and the velocity of the fluid, since the longer and rougher

the pipe, the greater the loss of friction, which is an important factor because it leads to decreased efficiency, increased energy costs, and equipment wear **[50]**.

I.3.4.2. Acceleration losses

Acceleration losses in fluidization refer to the pressure drop that occurs when a fluid accelerates due to changes in the system, such as an increase in temperature or a change in cross-sectional area. Acceleration losses can be large, especially in some cases, such as when the layer is subject to corrosion or particle attrition. Understanding this is important. Side is necessary to improve the performance of the bed **[51].**

I.3.4.3. Expansion losses

The term expansion losses refers to the pressure drop that occurs as a result of the expansion of the fluid as it passes through the fluidized bed. This expansion occurs due to the increase in the volume of the fluid because it raises the particles in the layer, which reduces the density of the fluid and increases its velocity. Therefore, it contributes to the overall pressure drop, but it is usually small compared to the other components of the pressure drop **[52]**.

I.4. Experimental Techniques for Pressure Drop Measurement

I.4.1. Overview of experimental methods for measuring pressure drop in fluidized beds

The experimental methods used to measure pressure drop in fluidized beds are considered extremely important for understanding fluidized bed behavior and for obtaining efficient fluidized bed designs. The most famous experimental methods for

measuring pressure drops are the following:

I.4.1.1. Pressure sensors

The pressure drop across the fluidized bed is measured using a differential pressure sensor, which measures the pressure difference between two points in the bed. We can do this by installing two pressure sensors at different heights in the belt as shown in Figure I.7 and connecting them to a differential pressure sensor that measures the pressure difference between the two sensors and uses it to calculate thepressure drop across the bed when carrying out the measurement process using this type, it is very important to take into account the pressure range and accuracy required for the application to choose the appropriate type to obtain the best results. For example, when the

expected pressure drop is several bars, we use a pressure sensor with a range of several bars. In addition to all this, the pressure sensor must have a high enough response frequency to capture pressure fluctuations accurately.

In general, the use of pressure sensors to obtain pressure drop measurements in the fluidized bed can provide valuable insights into the fluid dynamics of the bed and help improve bed performance. Still, it is important to carefully consider the selection of sensors, their installation, and measurement techniques to obtain accurate, highly accurate documented results **[53,54]**.

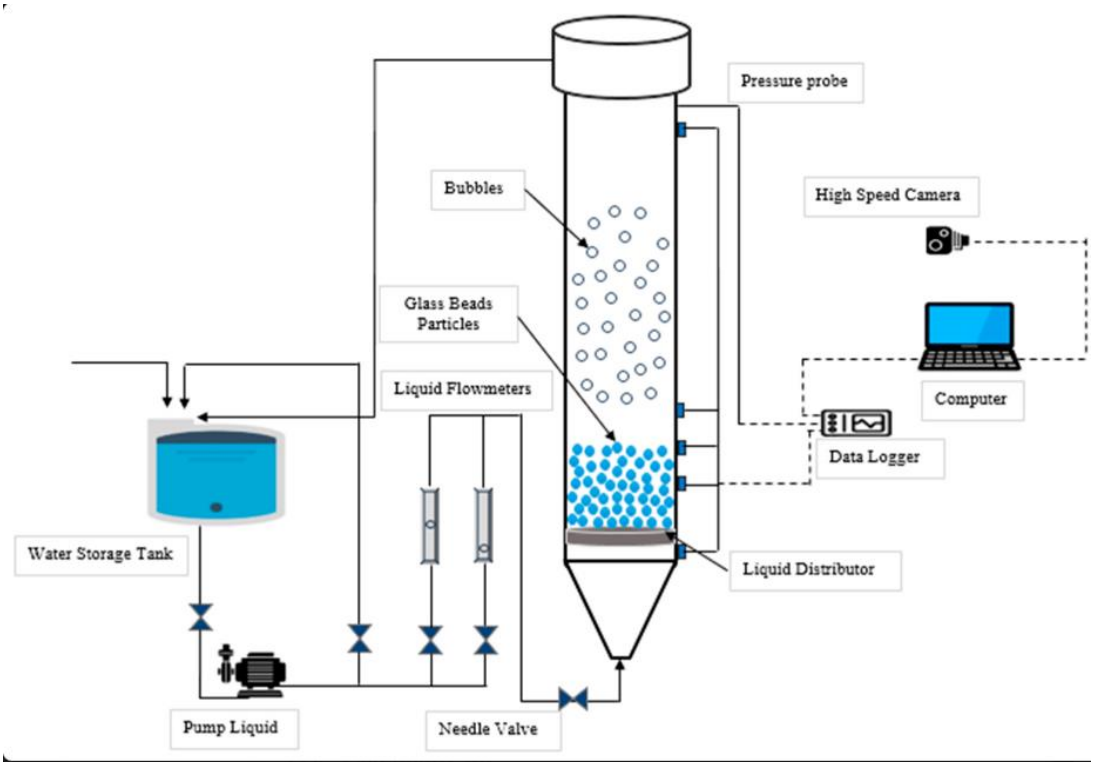


Figure I. 7. Layout reviews installing pressure sensors on the bed **[55]**

I.4.1.2. Manometers

Manometers can be used to calculate the pressure drop in the fluidization process. Manometers are instruments used in science to measure the pressure of gases. The open manometer measures the pressure of the gas and compares it with the atmospheric pressure. An open manometer has an immiscible fluid arranged in a U-shaped tube such that its density is more compared to the fluid flowing. One end is connected to the point where pressure will be measured and the other end is

connected to the pipe near the point of interest. Pressure difference measurement in fluidization using manometers provides engineers and researchers with adequate information to optimize fluidized bed use and scheduling **[56]**.

I.4.1.3. Pitot tubes

It is measured by measuring the static and dynamic pressure differences with a pitot tube. The fluid under motion creates what is known as dynamic pressure while the fluid under rest has static pressure. A typical pitot tube is made of a tube that enters into the flow of fluid with an outlet facing forward in the direction of flow. This opening measures the total pressure sums of both static and dynamic pressures. On the side of the tube, at right angles to it, there is another opening where we measure static pressure the remaining part which can be obtained by subtracting the static pressure from total pressure is referred to as dynamic pressure, using the Bernoulli equation this velocity can be calculated. It is very important to take into account that Pitot pipes are affected by freezing, which may lead to errors in the pressure measurement process. Therefore, it is very important to ensure regular maintenance of Pitot pipes properly and to protect them from freezing under cold temperatures **[57]**.

I.4.2. Considerations for experimental setup and data acquisition

Many considerations must be taken into account for experimental setup and obtaining data, including **[45,58]**:

- Choosing the appropriate membranes for the base, which when we choose, we choose them suitable for pressure;
- To obtain and store data, for this purpose we can use a Central Processing Unit (CPU) processing unit and a graphic interface program such as lab view which we will use to read and store data;
- It should also be taken into account that most of the pressure drop fluctuations appear at the bottom of the fluidized bed;
- The Froude number can be used to measure density, generally used for liquid-solid fluidization;
- We repeat the experiment several times to obtain the best and most accurate results.

There are many considerations, and what we mentioned in this context is just a glimpse of them.

I.4.3. Case studies highlighting experimental investigations of pressure drop in fluidized systems

Many different experimental studies have conducted experiments on pressure drops in fluidized systems, with different years. We will take a sample of these studies and organize them in Table I. 1 in which we will mention the name of each scientist along with the year in which he experimented and mention the most prominent results obtained**.**

Table I. 2. Several experimental tests for pressure drop in fluidization, with most prominent results.

References	year	The most prominent results
Pillay **[59]**	1983	They explored multistage fluidization and made correlations between pressure drop and solids holding time with relative velocities, Froude number, and particle and perforation characteristics.
Chakrabarti **[60]**	2005	Pressure gradient measurements were made for different combinations of phase superficial velocities ranging from 0.03-2 m/s.
Hashizume **[61]**	2008	A calculation method for predicting the pressure drop in riser tubes could reproduce almost all data with an accuracy of 20%.
Hashizume **[62]**	2009	A calculation method for predicting the pressure drop in the riser could reproduce almost all the data with an accuracy of 20%.
Zakeri **[63]**	2012	The selected software in general gives reliable predictions of pressure drop up to an F-factor of about 3 Pa 0.5 at high liquid loads
Eain **[64]**	2013	The addition of a second immiscible phase is accompanied by an increase in pressure drop relative to the single-phase flow case.
Hamad **[65]**	2017	The pressure drop increases with higher volumetric qualities for the cases of constant water flow rate.
Peng **[45]**	2022	The flow resistance coefficient experiences a decrease with the increase in the modified particle Reynolds number and densimetric Froude number.

I.5. Pressure drop models

The development of practical and theoretical models for calculating pressure drop has undergone many modifications since its inception. As science advances, our understanding of the

various factors affecting it increases. We will present some examples of the most important models in this field, including:

I.5.1. Forchheimer correlation

It is an equation developed by the scientist Forchheimer to describe and calculate pressure drop in porous media, the experimental correlation was developed using analogy with pipe flow with coefficients as correction factors to calculate viscosity and also inertial terminology **[66]**. The equation of this model can be written as follows:

$$\frac{\Delta P}{H} = -\left(\frac{\mu_f}{K}\mathbf{U} + F\frac{\rho}{\sqrt{K}}\mathbf{U}^2\right) \quad \text{(I.4)}$$

Where:

ΔP: Pressured drop (Pa).

H: Bed's height (m).

μ_f: Dynamic viscosity of the fluid (kg/m.s).

U: Average velocity of the flow (m/s).

ρ: Fluid density (kg/m^3).

F: Forchheimer coefficient (m). Which is calculated by the relationship:

$$F = \beta\sqrt{K} \quad \text{(I.5)}$$

K: Permeability (m^2). Which is calculated by the relationship:

$$K = \frac{d^2.\varepsilon^3}{36k(1-\varepsilon)^2} \quad \text{(I.6)}$$

Where also:

β: Inertial resistance coefficient (-).

k : Carman-Kozeny constant (-).

ε: Porosity (-).

d: Particle diameter (m).

I.5.2. Blake–Kozeny equation

It is a mathematical equation that describes the relationship between pressure drop and flow velocity in different media consisting of spherical particles that share a uniform size **[67]**. It is represented by the relationship:

$$\frac{\Delta P}{H} = 150\frac{(1-\varepsilon)^2}{\varepsilon^3}\frac{\mu_f}{{d_p}^2}U \qquad \text{(I.7)}$$

Where:

ΔP: pressured drop (Pa).

H: bed's height (m).

ε: porosity (-).

μf: dynamic viscosity of the fluid (kg/m.s).

U: flow velocity (m/s).

d_p: particle diameter (m).

I.5.3. Burke–Plummer equation

It is a relationship that describes the relationship between pressure drop and fluid velocity, where the pressure drop is directly proportional to the square of the fluid velocity. It can be used at high flow speed (or high Reynolds number) **[67]**, and is described by the equation:

$$\frac{\Delta P}{H} = 1.75\frac{(1-\varepsilon)}{\varepsilon^3}\frac{\rho_f}{d_p}U^2 \qquad \text{(I.8)}$$

Where:

ΔP: pressured drop (Pa).

H: bed's height (m).

ε: porosity (-).

ρf: fluid density (kg/m^3).

U: flow velocity (m/s).

d_p: particle diameter (m).

I.5.4. Ergun equation

The original Ergun equation was proposed in 1952 through a direct combination of the Blake–Kozeny equation and the Burke–Plummer equation. It is considered a very satisfactory equation for predicting pressure drop in Newtonian flow. The equation was considered comprehensive because its right term is related to the viscous effect, while the left term is concerned with the loss of kinetic energy **[67]**. It is represented by the equation:

$$\frac{\Delta P}{H} = 150\frac{(1-\varepsilon)^2}{\varepsilon^3}\frac{\mu_f}{{d_p}^2}U + 1.75\frac{(1-\varepsilon)}{\varepsilon^3}\frac{\rho_f}{d_p}U^2 \qquad \text{(I.9)}$$

Where:

ΔP: pressured drop (Pa).

H: bed's height (m).

ε: porosity (-).

ρf: fluid density (kg/m^3).

μf: dynamic viscosity of the fluid (kg/m.s).

U: flow velocity (m/s).

d_p: particle diameter (m).

In short, the Forchheimer correlation is an extension of Darcy's law and is used in turbulent media and includes viscosity and inertia, and the Blake–Kozeny equation is related to a specific surface area and is used especially in spherical particles, while the Burke–Plummer equation is derived from experimental data and takes into account the size of the particles, their density, and layer height, and in The last, Ergun equation, includes the two-part effect of viscosity and inertia, and is the most widely used. That is, we can say although all of these equations explain pressure drop in fluidized systems, they differ in terms of their theoretical underpinnings, presumptions, and suitability for various flow regimes and particle properties. Based on the unique parameters and needs of their system, researchers and engineers select the best equation.

I.6. Application of pressure drop analysis in industrial processes

Pressure drop analysis is one of the most important things that must be taken into consideration when talking about fluidization processes in various industrial applications. Contributes to the selection of appropriate conditions and process equipment. Among its most important applications, and based on what you discussed previously, especially the relationship between it and other parameters such as bed length, fluidization speed, etc. We can conclude the following applications:

- Fluidized bed r eactor design;

- Identification of flow regimes;

- -Scaleup and process optimization;

- Troubleshooting and maintenance;

- Optimization of fluidization conditions;

- Bed material selection.

I.7. Conclusion

So, in general, and as a summary of what we said, the study of pressure drop in the phenomenon of fluidization brings many, many benefits to us in various industries, in economic and environmental aspects in general, and in the field of chemical engineering in particular.

We also clarified the phenomenon of fluidization and focused on pressure drop in terms of the factors and parameters affecting it and the different ways of measuring it, arriving at the most important models that dealt with it and expanding our understanding and understanding of it.

Chapter II: Generalize about artificial intelligence

II.1. Introduction

The basic principle of artificial intelligence (AI) is to build an intelligent machine that thinks like a human **[68]**.

The origins of artificial intelligence go back to ancient greek mythology, which says that a mechanical man can mimic human behavior. However, it seems that the quest for this became a reality when many scientists from different disciplines such as neuroscience and computer science came together during the war. The second global revolution to reach smart machines **[68]**.

In this chapter, we will talk in general about artificial intelligence, define it, and mention the most important basics in it, down to the algorithms used in our work to gain a greater understanding of this distinctive field.

II.2. Historical Review

Since time immemorial, humans have tried to find techniques to make their daily lives easier and reduce tasks. Perhaps the historical point in the transformation of human life occurred when ancient humans discovered fire, as cooked foods are easier to digest and therefore require fewer neurons, specifically in the lower part of the brain. Which controls digestion processes, as Figure II.1 shows, thus saving the body's energy.

As we know, humans are at the top of the food chain, and therefore humans have always built tools that have an impact on human development and multiply human power. In ancient times, it surpassed the ingenious machine of Archimedes in Alexandria in particular, where in 150 AD he was able to build a steam engine that could open the door of the temple alone, surpassing all human muscles. Moreover, before it specifically in 1200 BC, the Antikythera machine was built, which had the ability to perform Advanced astronomical calculations including predicting eclipses. These and other examples show that the foundations for building automation and systems that later developed and became the cornerstone of computer science and artificial intelligence were laid two thousand years ago **[69].**

It can be noted that the first computers were not far from the machines of ancient times. Perhaps the most notable difference is the ability to create logical operations that combine "and" and "or". Perhaps the element that revolutionized technology is the transistor, thanks to which computers were made smaller and smaller, and thus the ability to perform more complex

mathematical operations, and the human desire to reach greater development continued, as in 1952, Alan Turing, one of the founders of computing, created a program that could play chess, very close to current systems.

The actual leap in this field occurred in the year 1956 when ten high-ranking people met to define artificial intelligence, including John McCarthy, Marvin Minsky (one of the founders of the artificial intelligence laboratory at the Massachusetts institute of technology), and Herbert Simon (winner of the Nobel Prize in economics in 1978, and the inventor of rationality). Claude Shannon (inventor of information theory). One of the most important goals of this symposium was to define intelligence using computer tools, to be one of the cornerstones of the world of artificial intelligence **[70].**

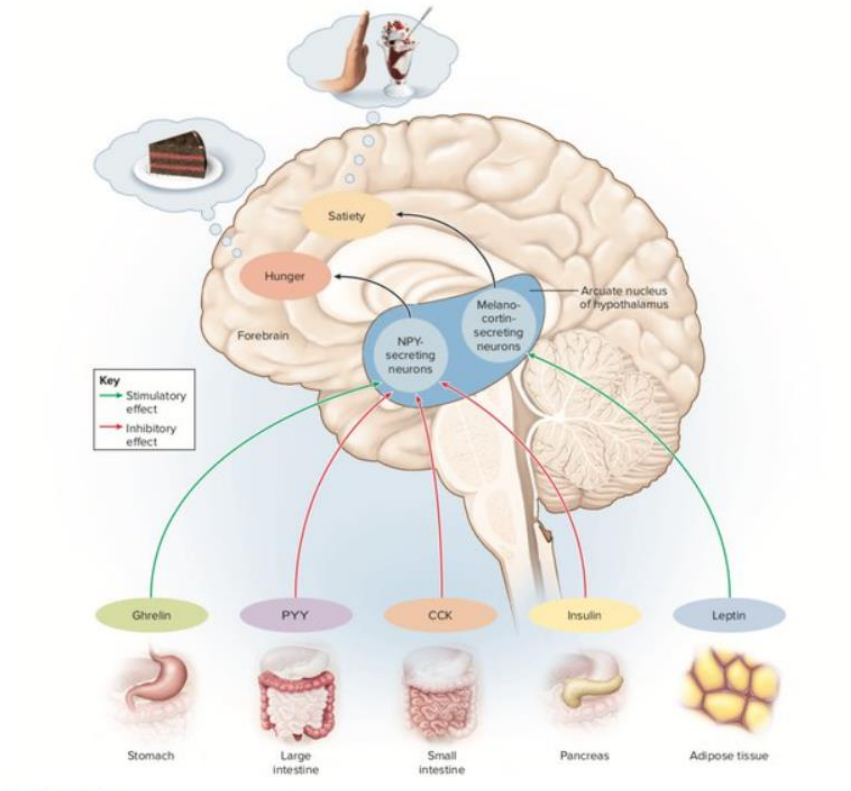


Figure II. 1. The parts of the brain responsible for hunger **[71]**

II.3. Definition of Artificial Intelligence

Defining artificial intelligence is a complex matter due to many difficulties, such as that the field is so broad that it cannot be confined to a specific research field. That is, it is a multidisciplinary program that, in its beginnings, aimed to imitate human cognitive processes. However, with modern development, the goal has become to develop systems that can solve problems much better than humans, meaning that as a summary of all of the above **[72],** we can summarize it in the form of the following two definitions:

Definition 1: In which we can summarize Artificial Intelligence (AI) as a set of algorithms that process a set of information or data related to tasks in a manner similar to and mimicking those that a human might undertake.

Definition 2: In which we can say that the intelligent system is therefore an artificial intelligence system in which the components are divided into two parts:

- The physical part that contains electronic equipment such as programmable electronic cards, computers, etc.

- The computerized part consists of several programs that can process information of different types and forms.

Hence, we note that artificial intelligence is an expression of a link between many disciplines such as computer science and mathematics (logic, analysis, optimization, probability, linear algebra) and many other fields.

II.4. The main classification of AI

The classification of artificial intelligence has faced many difficulties due to the many fields it falls into and the classifications differ according to the advantages provided and the goals sought from it. Perhaps the most prominent classifications are those related to simulating human activities such as movement, learning, thinking, awareness, and creativity. Accordingly, **[72,73]** artificial intelligence has been classified into two main areas:

II.4.1. Weak artificial intelligence

We can say that it is the complete imitation of observed human behavior in which the behavior is reproduced accurately without any addition or alteration using computer programs, and it is a classification in which there is no possibility of evolution.

II.4.2. Powerful artificial intelligence

It is a type in which human behavior is imitated while simulating the continuation of learning and the accumulation of knowledge more and more, and therefore it is more complex than the first. In this type, for example, algorithms develop and gradually emerge from the framework in which they were placed by their authors or developers.

We can see the main classification of artificial intelligence in the following Figure II.2.

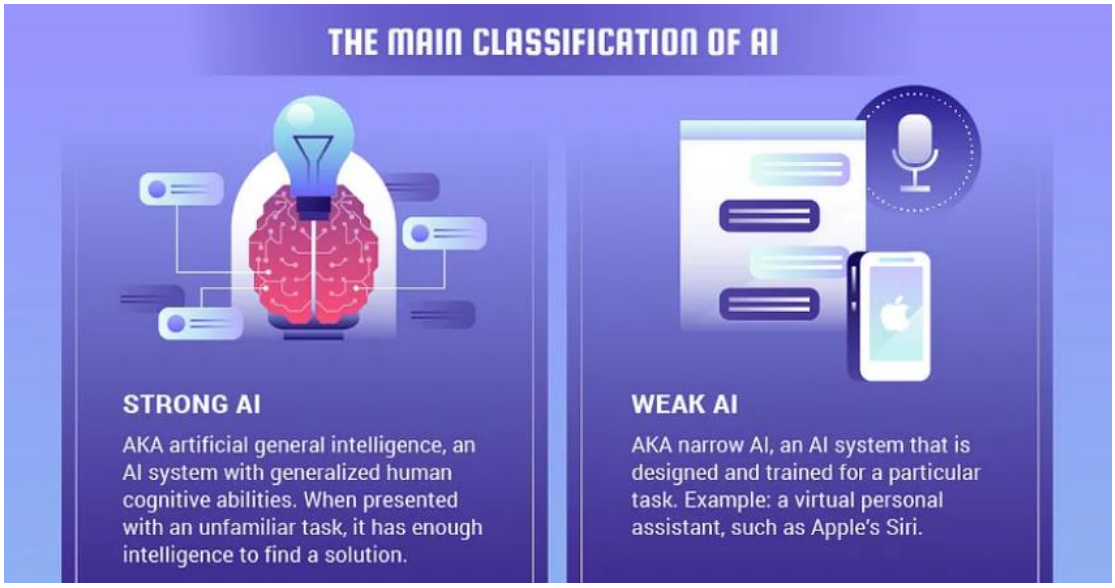


Figure II. 2. The main classification of AI **[74]**

II.5. Types of Artificial Intelligence

As we mentioned previously, because artificial intelligence has become part of almost all areas of our lives as Figure II.3 shows, we can divide it into many sub-fields, including:

II.5.1. Machine learning

Machine learning is the field that, as its name indicates, addresses the aspect in which we build computers that learn and improve automatically through experimentation and learning. This

field is considered one of the most important, growing, and widespread fields of artificial intelligence these days, and we can say that this field is the link between computer science and statistics. The paradigm shifts and major development in this field occurred when it was linked to new learning algorithms and theories, allowing for evidence-based decision-making. Today this field is included in science, technology, commerce, learning, marketing, and many others **[75].**

II.5.2. Natural language processing

We can say that it is a set of mathematical operations for tools for the automatic analysis and representation of human languages with theoretical motives, that is, it is based on textual analysis, and therefore it requires a deeper understanding of the nature of language using machines, the most prominent examples of which are: retrieving information from the Internet, compiling it, and answering the questions it has. It is based primarily on algorithms that depend on the textual representation of web pages, dividing parts, verifying writing, and analyzing the level of each word. Therefore, one of its most prominent problems is dealing with paragraphs and extracting benefits from them, as its ability in this field is limited **[76].**

II.5.3. Speech

Processing and understanding human speech is one of the challenges facing artificial intelligence, and there are many applications in this field, such as speech recognition systems for dictation, speech production for automated advertising, including human-computer interface (HCI), and voice-activated transactions. One of the challenges in this field is processing the audio stream and dividing it into separate words **[77].**

II.5.4. Planning

In this field, we mean automatic planning, which is the mechanism responsible for choosing the correct sequence of procedures to complete a specific task in the best way. This is done by finding the best appropriate representation of the problem area, or in other language we can say it is a series of steps consisting of the best path that takes by dealing with the initial state until it reaches the target state, and after that, we take the coordinates of the optimal path in terms of time and place to run the algorithm **[77].**

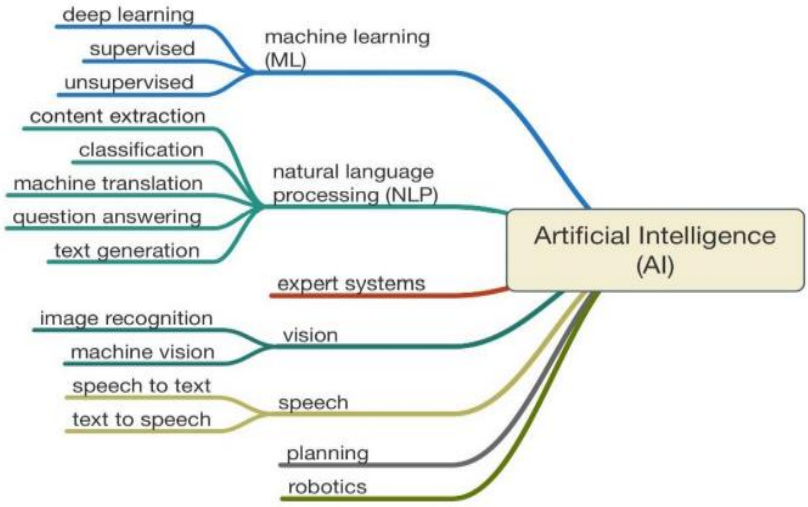


Figure II. 3. Types of artificial intelligence **[78]**

II.6. AI algorithm

II.6.1. Definition of AI algorithm

Artificial intelligence algorithms are about giving machines the ability to learn and study data and make appropriate decisions by giving them a set of instructions or rules, in other words, giving the machine the ability to think like humans and give it the intelligence to perform a set of applications such as recognizing patterns, understanding natural language, and solving problems **[79].**

II.6.2. AI algorithms work

One of the things that should be clear to everyone is that artificial intelligence algorithms are, by their nature, more complex than ordinary algorithms. Artificial intelligence algorithms generally neglect learning, as they receive training data through which they learn so that they can later make predictions, make decisions, etc., and the method of obtaining them is considered. This data and dealing with it is the main difference between the different types of artificial intelligence algorithms.

That is, in general, artificial intelligence takes classified or unlabeled training data provided by developers or that it collects itself, processes that data and uses it to learn and develop itself, and then performs the tasks assigned to it using the training data as a basis. Here it is worth noting

that some artificial intelligence algorithms They are taught to develop and improve their data on their own while other algorithms require human intervention **[80].**

II.6.3. Types of Artificial Intelligence Algorithms

Many categories of classification of artificial intelligence algorithms differ in how they are trained and how they work, including the following three main categories:

II.6.3.1. Reinforcement learning

They are artificial intelligence algorithms that learn by receiving panic responses after performing their work, usually in the form of a "reward".

We can say that reinforcement algorithms usually consist of two parts: the agent that performs the action and the environment in which the action is performed. The cycle begins when the environment sends a "status" signal to the agent. The agent then performs a specific action within the environment. After executing the action, the environment sends a signal. The reward for the agent is either "positive" or "negative" depending on the event. Accordingly, the agent evaluates the last action and updates the situation. The cycle is repeated until an end signal is sent from the environment **[81].**

II.6.3.2. Unsupervised learning

As its name indicates, this type refers to algorithms in which there is no teacher. In this type, unclassified and unlabeled data is presented to the algorithm, and based on the characteristics and features of that data and the relationships between the various points, it learns the data and implements the appropriate action based on training on the characteristics and features of similar data, and it is used. Mainly for clustering **[82].**

II.6.3.3. Supervised learning

Supervised learning is, as its name indicates, adapted from the student's learning in the presence of a teacher or an expert. It is considered the most important and widely used methodology in machine learning these days, and this type of algorithm works by mapping input variables X, and output variables Y to predict invisible data outputs.

Building an already supervised learning algorithm requires a team of experts, technologists, and others to review the results, and data scientists to test the accuracy of the results **[83].** The most famous types of supervised learning algorithms are Classification and Regression where All of

them can either be used for classification or regression, or both. Each one is defined as follows **[80]:**

- **Classification :** is the use of binary (0 = no, 1 = yes) to produce an either/or conclusion. Thus, something will only ever be categorized by the algorithm as one or the other, never as both. Multi-class categorization pertains to the arrangement of data into predetermined categories or types that are pertinent to a certain requirement.
- **Regression:** a real number-either a round number or a decimal point—will appear after the output. The algorithm typically uses the points from the dependent and independent variables to estimate a possible other result (either forecast or generalized estimate).

There are a lot of supervised learning algorithms, including:

II.6.3.3.1. Decision Tree

One of the most popular approaches for representing classifiers in data classification is the use of decision tree classifiers. The topic of expanding a decision tree from existing data has been studied by numerous researchers from a variety of disciplines and backgrounds, including statistics, machine learning, and pattern recognition. In many domains, including text classification, medical disease analysis, smartphone user classification, photos, and many more.

Where, with this algorithm, the methods used are taken, the paint set and the results achieved are expressed in leaves **[84].**

II.6.3.3.2. Support Vector Machines

It was introduced by Vapnik to solve classification and regression problems based on statistical learning theory **[85],** machine learning is a branch of artificial intelligence whose principle is developing algorithms to enable a machine to learn and perform various tasks **[86],** we have turned to SVM techniques because ANN models contain some obvious drawbacks, such as local minima, over-fitting problems **[87],** The data set in it is expressed by the equation $\{(x_i, y_i), i = 1,2, \dots, N\}$ Where x_i and $y_i$respectively indicate ith element in n-dimensional space and the real-valued output and N the number of data patterns. And it is expressed support vector regression (SVR) by the equation **[87]:**

$$f(x) = \langle w, x \rangle + b \qquad \text{(II.1)}$$

Where w and b stand for the regression function's weight vector and intercept, respectively. Next, the following regularized risk function is minimized in order to create the SVM regression problem:

$$R(f) = \frac{1}{N}\sum_{i=1}^{N} L(f(x_i) - y_i) + \frac{1}{2} \parallel w \parallel^2 \qquad \text{(II.2)}$$

Where:

$$L(f(x) - y) = \begin{cases} \parallel L(f(x) - y) \parallel - \varepsilon, & \text{if } |f(x) - y| \geqslant \varepsilon \\ 0 & \text{otherwise} \end{cases} \qquad \text{(II.3)}$$

A loss function that is ε-insensitive, where ε is a precision parameter that denotes the radius of the tube surrounding the regression function, f(x). We can find a function that fits the present training data with a deviation smaller than or equal to e by substituting equation (II.3) into (II.2). Rephrasing the SVM regression optimization problem as:

$$\text{minimize } \frac{1}{2} \parallel w \parallel^2 + C \sum_{i=1}^{N} (\xi + \xi^*) \qquad \text{(II.4)}$$

It is contingent upon the limitations listed below:

$$\text{s.t.} \begin{cases} \mathrm{y_i} - \langle w, x_i \rangle + b \leqslant \varepsilon + \xi_i \\ \langle w, x_i \rangle + b - \mathrm{y_i} \leqslant \varepsilon + \xi_i^* \\ \xi_i, \xi_i^* \geqslant 0 \\ i = 1,2, \ldots, N \end{cases} \qquad \text{(II.5)}$$

Where constant C indicates the positive regularization constant, which performs the function of determining the trade-off between generalization ability and accuracy in the training data, ε indicates the degree of tolerance to errors in the gap between real values and the associated boundary values of the ε-tube is represented by the positive slack variables ξ_i and ξ_i^*. The following function can then be maximized using the optimization method to derive a dual problem:

$$\text{maximize } -\frac{1}{2}\sum_{i,j=1}^{N} (\alpha_i - \alpha_i^*)(\alpha_j - \alpha_j^*)(x_i, x_j) - \varepsilon \sum_{i=1}^{N} (\alpha_i + \alpha_i^*) + \sum_{i=1}^{N} y_i(\alpha_i - \alpha_i^*) \qquad \text{(II.6)}$$

With the constraints:

$$\text{s.t.} \begin{cases} \sum_{i=1}^{N} (\alpha_i - \alpha_i^*) = 0 \\ 0 \leqslant \alpha_i \leqslant C \\ 0 \leqslant \alpha_i^* \leqslant C \\ i, \mathrm{j} = 1,2, \dots, N \end{cases} \quad \text{(II.7)}$$

Where the Lagrange multipliers α_i and α_i^* are acquired by solving a quadratic program. The SVM for fitting functions that were produced using the maximizing function indicated above is therefore provided as follows:

$$f(x) = (\alpha_{\mathrm{i}} - \alpha_{\mathrm{i}}^*)\langle x_i, x\rangle + b \quad \text{(II.8)}$$

In the dual space, the SVM regression function is finally obtained as equation (II.9):

$$f(x) = (\alpha_i - \alpha_i^*)K(x_i, x) + b \quad \text{(II.9)}$$

When a kernel function K (xi, x) that satisfies Mercer's requirements is given. Support vectors (SVs) are sample points that appear in equation (II.9) with non-zero coefficients. The Radial Basis Function (RBF) with width c is the often-used kernel function unless otherwise noted. Here is how the RBF is defined:

$$K(x_i, x_j) = \exp(-\gamma \|x_i, x_j\|), (\gamma > 0) \quad \text{(II.10)}$$

The three free hyper-parameters C, ε, and γ that were previously defined have a significant impact on the generalization performance of SVR. Where indicate penalty parameters, coefficient of non-sensitivity, and The RBF width parameter respectively. Figure II.4 shows the general form of the SVR representation.

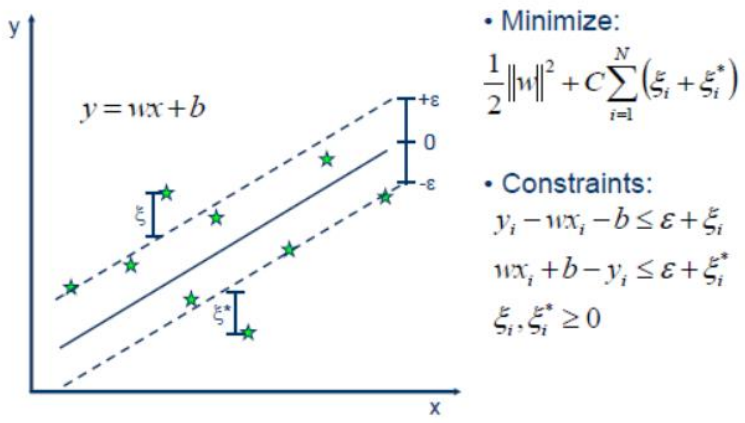


Figure II. 4. The form general of SVR **[88]**

II.6.4. Meta-heuristic algorithms

II.6.4.1. Particle swarm optimization

It is one of the Swarm intelligence algorithms that are a large branch of artificial intelligence **[89],** The algorithm is based on the behavior of flocks of birds when searching for food sources. It's a popular optimization algorithm due to its simplicity and use in a wide range of applications. It's considered one of the oldest and most well-known algorithms in the field because of its ease and possibility of use in various applications **[90].** It was presented and detailed for the first time in 1995 through two papers **[91,92]**, One of the most notable drawbacks is that it's easy to fall into local minimums and encounter convergence problems **[93]**, Many academic articles have talked about hybridization and improvement of the meta-variables used in them, including the effectiveness of their various methods and applications **[89].** Some articles discuss its most prominent challenges **[94].**

As for the structure of the standard algorithm, in it, a swarm of particles periodically updates their positions first so that the algorithm cansearchas necessary to reach the best solution. As for the movement of particles, each particle moves towards its previous best position (P_{best})and the bestgloballocation (g_{best}) movement is described by the equations **[89]**:

$$\mathbf{p}_{\text{best}\,i}^{t} = \mathbf{x}_i^* \mid f(\mathbf{x}_i^*) = \min_{k=1,2,\ldots,t}\left(\{f(\mathbf{x}_i^k)\}\right) \qquad \text{(II.11)}$$

where $i \in \{1,2,\ldots,N\}$, and

$$\mathbf{g}_{\text{best}}^{t} = \mathbf{x}_{*}^{t} \mid f(\mathbf{x}_{*}^{t}) = \min_{\substack{i=1,2,\ldots,N \\ k=1,2,\ldots,t}} \left(\{f(\mathbf{x}_{i}^{k})\}\right), \tag{II.12}$$

Where i refers to each individual particle,t is the current iteration number, f is the function or goal for which optimization (minimization) is to be made, **x** is the position vector (or a potential solution), and N is the number of particles in the swarm. The following equations describe velocity **v** and position **x** for each iteration t+1:

$$\mathbf{v}_{i}^{t+1} = \omega \mathbf{v}_{i}^{t} + c_1 \mathbf{r}_1 (\mathbf{p}_{\text{best}}^{t} - \mathbf{x}_{i}^{t}) + c_2 \mathbf{r}_2 (\mathbf{g}_{\text{best}}^{t} - \mathbf{x}_{i}^{t}) \tag{II.13}$$

$$\mathbf{x}_{i}^{t+1} = \mathbf{x}_{i}^{t} + \mathbf{v}_{i}^{t+1} \tag{II.14}$$

Where v is a velocity vector, ω it is the function that expresses the weight of inertia, and in the algorithm, it is used to reach an equilibrium between local exploitation and global exploration $\mathbf{r}_1$, and $\mathbf{r}_2$ they are random vectors uniformly distributed within the domain $[0,1]^D$ (where D is the dimensionality of the search space or the magnitude of the current issue), $c_1$and c_2 these positive constants are referred to as "acceleration coefficients". Figure II.5 shows the simulation of the process of choosing the best location for a flock of birds.

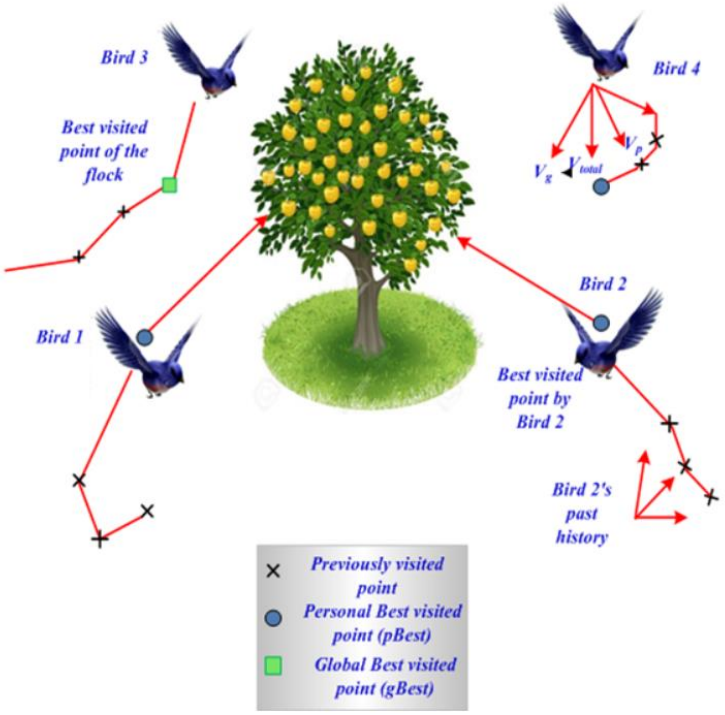


Figure II. 5. The conceptual framework for identifying the best visit point in a swarm **[95]**

II.6.4.2. Dragonfly algorithm

It was first introduced in 2016 and was inspired by static and dynamic dragonfly swarms' behaviors **[96],** it was inspired by the cluster behavior of dragonflies, specifically during hunting and migration, and is divided into two swarms: static and dynamic. The static swarm is the hunting swarm, where dragonflies gather in small groups and fly in a limited area back and forth to hunt prey. The second dynamic swarm describes the case of moving long distances in one direction. To express it in another language, the two phases are called the exploration phase and the exploitation phase, where in the case of the first swarm, movement in a limited area represents the exploration phase of the optimization algorithm, while flying in one large swarm in one direction is useful for exploitation **[97].** Figure II.6 shows the five basic actions of a dragonfly. The behavior of any swarm follows the principles outlined by Reynolds **[98]:**

Separation, alignment, and cohesion. To imitate the natural behavior of dragonflies, the members of the group are attracted to food and get distracted by external threats, in addition to what is mentioned above. Mathematical models are used to update the locations with every iteration, which can be summarized in the following manner:

(1) Separation: The goal of this process is to prevent collision between each member of the group with other individuals and is expressed by equation (II.15):

$$S_i = -\sum_{j=1}^{N} X - X_j \qquad \text{(II.15)}$$

Where X displays the site of the current individual,X_j represents the site of the jth individual in close proximity, and N The number of individuals hovering around.

(2) Alignment : The meaning of which is that all individuals in the same group move with the same speed, and itis expressed by equation (II.16):

$$A_i = \sum_{j=1}^{N} V_j/N \qquad \text{(II.16)}$$

Where V_j displays the velocity of the j-th neighboring individual.

(**3) Cohesion**: This indicates the tendency of the group to form a single bloc through the tendency of the individual to move towards the center of the group, and itis expressed by equation (II.17):

$$C_i = \left(\sum_{j=1}^{N} X_j / N \right) - X \quad \text{(II.17)}$$

(4) Attraction: to where food is located by equation (II.18):

$$F_i = X^+ - X \quad \text{(II.18)}$$

Where X^+ points to the site of the food source.

(5) Distraction: to describe avoiding and going away from enemies by equation (II.19):

$$E_i = X^- + X \quad \text{(II.19)}$$

Where X^-pointing to the site of the enemy.

Previous models describe the behavior of dragonflies in nature with some of their usual behaviors, and for the simulation to be comprehensive, the location of the dragonfly is updated with each iteration by the step vector ΔX expressed by equation (II.20):

$$\Delta X_{t+1} = (sS_i + aA_i + cC_i + fF_i + eE_i) + w\Delta X_t \quad \text{(II.20)}$$

Where $s, a, c, f,$ and e indicate and respectively the separation weight, the alignment weight, cohesion weight, the food factor, and the enemy factor, and also $S_i, A_i, C_i, F_i,$ and E_i indicates to and respectively the separation, the alignment, the cohesion, s the food source and the enemy's location of the i-th individual. w is the weight of inertia, and t is the iteration counter, after performing the calculations received with the step vector, the position vector is expressed by equation (II.21):

$$X_{t+1} = X_t + \Delta X_{t+1} \quad \text{(II.21)}$$

If the dragonfly was moving in the absence of other individuals in the vicinity, DA uses random movement or Lévy flight **[99]**, which is used to improve random behavior and exploration in search of solutions, where the dragonfly's location is updated by equation (II.22):

$$X_{t+1} = X_t + \text{ Lévy } (d) * X_t \quad \text{(II.22)}$$

d is the dimension of the position vectors. The Lévy flight is calculated as follows by equation (II.23):

$$\text{Lévy}\,(x) = 0.01 * \frac{r_1 * \sigma}{|r_2|^{\frac{1}{\beta}}} \qquad \text{(II.23)}$$

Where r_1 and r_2 are two random numbers in [0,1], β is a constant, and σ is calculated as follows by equation (II.24) and (II.25):

$$\sigma = \left(\frac{\Gamma(1+\beta) * \sin\left(\frac{\pi\beta}{2}\right)}{\Gamma\left(\frac{1+\beta}{2}\right) * \beta * 2^{\left(\frac{\beta-1}{2}\right)}} \right)^{\frac{1}{\beta}} \qquad \text{(II.24)}$$

$$\text{Where } \Gamma(x) = (x-1)\,! \qquad \text{(II.25)}$$

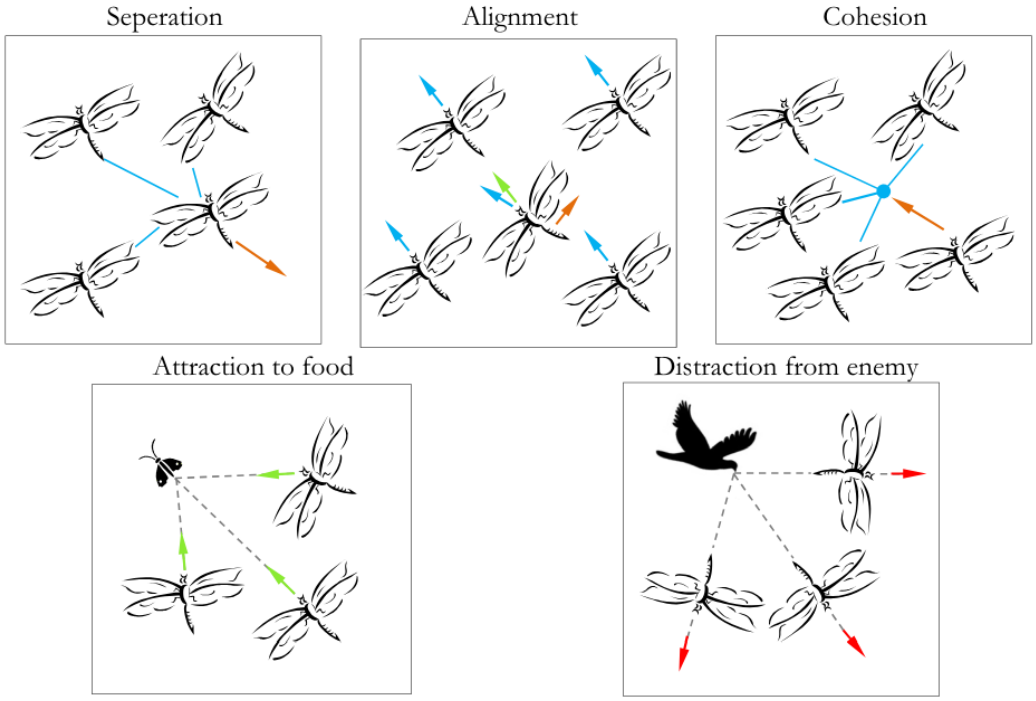


Figure II. 6. Simple correction patterns amongst members of a swarm **[96]**

II.6.4.3. Grey wolf optimizer

It was first discussed in 2014 by Mirjalili **[100],** An algorithm that was inspired by the behavior of wolves. In the structure of the algorithm, the hierarchical relationship within a flock of gray wolves in the wild was simulated. The hierarchical behavior of wolves was simulated using four

types of wolves: alpha**(α)**, beta**(β)**, delta**(δ)**, and omega**(ω)**, which indicate, respectively, the best solution and the second best solution, the third best solution, and the last remaining best solutions **[101],** The algorithm includes four sections: social hierarchy, tracking, encirclement, and attack. As for the first section, it is the one we talked about. As for encirclement, the behavior of the target (the encircled prey) will be mathematically formulated as follows by equation (II.26) to (II.32):

If we say that $\vec{X}$ and $\vec{X}_p$ are respectively current position vectors of a grey wolf and the current prey position, the mathematical relationship will be as follows:

$$\vec{D} = \left|\vec{C} \cdot \vec{X}_p(t) - \vec{X}(t)\right| \quad \text{(II.26)}$$

$$\vec{X}(t+1) = \vec{X}_p(t) - \vec{A} \cdot \vec{D} \quad \text{(II.27)}$$

Where $\vec{A}$ and $\vec{C}$ represent the coefficient vectors and exploitation and exploration, respectively which is expressed in the form:

$$\vec{A} = 2\vec{a} \cdot \vec{r}_1 - \vec{a} \quad \text{(II.28)}$$

$$\vec{C} = 2 \cdot \vec{r}_2 \quad \text{(II.29)}$$

Where components $\vec{a}$ are linearly decreased from 2 to 0, $\vec{r}_1$ and $\vec{r}_2$ are random vectors between the value [0,1], $\vec{A}$ random value represents the margin between -α and +α which lies within the boundaries of the field [-1,+1] which in the algorithm simulates attacking prey, where if $\left|\vec{A}\right|$<1, The current position of the prey will be adopted and the wolves will attack it. The algorithm considers vector $\vec{C}$ as the effect that arises when obstacles approach the prey in nature.

The previous equations describe the formula in its general form for the operation of the algorithm in its two stages, the search for the best location and the hunt, which was presented and explained by Mirjalili **[100]**. To create more flow and the best application of the algorithm, we can force each of the **α, β, δ,** and even other values **ω** wolves to update their location with each iteration according to the following formula:

$$\vec{D}_i = \left|\vec{C}_j \cdot \vec{X}_i - \vec{X}\right| (i = \alpha, \beta, \delta; j = 1,2,3) \quad \text{(II.30)}$$

$$\vec{X}_j = \vec{X}_i - \vec{A}_j \cdot \vec{D}_i (i = \alpha, \beta, \delta; j = 1,2,3) \quad \text{(II.31)}$$

$$\vec{X}(t+1) = \frac{\vec{X}_1 + \vec{X}_2 + \vec{X}_3}{3} \quad \text{(II.32)}$$

As a summary of everything that was talked about, alpha, beta, and delta are calculated according to the relationships explained, through which the best location for the prey is estimated through the three best solutions, and an update is made with each iteration **[101]**.

II.7. Conclusion

In conclusion to all of the above, we gave the most important basic points to give a first look at the basics of artificial intelligence, starting from its definition to some historical reviews, they also talked about the most important classifications of artificial intelligence and its basic types, all the way to algorithms, which alone are considered an integrated world of science, finally, arriving at an explanation and definition of the algorithms used in our work.

Chapter III

Experimental Study and Modeling of Pressure Drop in Fluidized Beds

III.I. Introduction

The accurate prediction of pressure drop in fluidized beds is crucial for various industrial processes, spanning from chemical engineering to environmental sciences. In recent years, Support Vector Regression (SVR) has emerged as a promising technique for modeling complex systems due to its ability to handle non-linear relationships and high-dimensional data effectively. However, enhancing the performance of SVR models remains a significant challenge, particularly in applications with intricate dynamics such as fluidized bed systems.

In response to this challenge, we have turned to metaheuristic optimization algorithms to enhance the capabilities of SVR in modeling pressure drop phenomena in fluidized layers within cylindrical and conical beds. Metaheuristic algorithms, such as Particle Swarm Optimization (PSO), Dragonfly Algorithm (DA), Grey Wolf Optimizer (GWO), and others, offer innovative solutions for optimizing model parameters and improving predictive accuracy.

This introduction sets the stage for exploring the utilization of SVR, both independently and in conjunction with metaheuristic optimization algorithms, to develop robust models for predicting pressure drop in fluidized bed systems in cylindrical and conical fluidized beds. Through this research, we aim to contribute to the advancement of predictive modeling in fluidized bed technology, enabling more efficient and reliable process design and optimization in various industrial applications.

III.2. Methodology

III.2.1. Data-set collection and pretreatment

In this study, we have collected a database consisting of 406 samples from various previous works on pressure drop in cylindrical and conical fluidized beds. 171 samples were collected for a cylindrical fluidized bed and 235 samples were collected for a conical bed. The samples were taken for several experiments with different bed dimensions and angles.

III.2.1.1. Normal model

For the normal model, nine parameters were selected as inputs namely the porosity of the bed (ε), the diameter of the particles inside the bed (d_p), the height of the bed (H), the density of the

bed particles (ρ_s), the density of the fluid used (ρ_f), the dynamic viscosity of fluid (μ_f), the diameter of the inner tube of the bed (D_0), in addition to the cos of the angle (Cosα), which is equal to one

for the cylindrical bed and calculated according to each bed for the conical bed and finally the fluidization velocity (U). One output is selected which is the pressure drop in the bed (ΔP). Table III.1 shows the range of different input and output parameters along with the units for each parameter used to build the model.

III.2.1.2. Dimensionless model

The dimensionless parameters selected to build the model aim to avoid converting units between different systems. This model consists of five dimensionless inputs which are Reynolds number, Archimedes number, pipe inner diameter/bed height, hydraulic diameter/particle diameter, cos of the angle (Cosα), and the only output is the Euler number. Table III.2 shows the range of different parameters we used to build the model. The following equations were used to calculate the input and output values from the normal form data. from equation (III.1) to (III.5):

$$\mathrm{Re} = \frac{d_p}{V_f} U \qquad \text{(III.1)}$$

Where V_f, it is kinematic viscosity(m²/s) .Which is calculated from the equation. Eq (III.2):

$$V_f = \frac{\mu_f}{\rho_f} \qquad \text{(III.2)}$$

$$\mathrm{Ar} = \frac{g . d_p^3 . \rho_f . (\rho_s . \rho_f)}{\mu_f^2} \qquad \text{(III.3)}$$

Where g it is the Earth's gravitational acceleration and is equal to 9.81(m/s²).

$$d_h/d_p = \frac{2.\varepsilon}{3.(1-\varepsilon)} \qquad \text{(III.4)}$$

$$\mathrm{Eu} = \frac{\Delta P}{\rho_f . U^2} \qquad \text{(III.5)}$$

Table III. 1. Data ranges (Normal model)

		Min	Max	Average
Inputs	**ε(-)**	0.240	0.636	0.434
	d_p(m)	0.566×10^{-4}	0.170×10^{-2}	0.530×10^{-3}
	H(m)	0.197×10^{-1}	0.390	0.153
	Cosα(-)	0.866	1	0.991
	ρ_s(kg/m^3)	1396	6700	1951.500
	ρ_f(kg/m^3)	1.127	1.214	1.166
	μ_f(kg/m.s)	0.170×10^{-4}	0.191×10^{-4}	0.185×10^{-4}
	D_0(m)	0.050	0.180	0.145
	U(m/s)	0.394×10^{-2}	1.966	0.491
Output	**ΔP(Pa)**	4.639	2613.180	1117.470

Table III. 2. Data ranges (Dimensionless model)

		Min	Max	Average
Inputs	**Re (-)**	0.153×10^{-1}	104.300	17.600
	Ar (-)	24.470	277635.700	14317
	D_0/H (-)	0.250	4.090	1.635
	d_h/d_p (-)	0.210	1.164	0.537
	Cosα (-)	0.866	1.000	0.991
Output	**Eu (-)**	156.460	647278.880	53350.360

III.2.2. Data division and model development

After various trials were conducted for the division of the test data from 15% to 35%, the suitable division was 20% for the test stage and 80% for the training stage. As for the four algorithms SVR, SVR-PSO, SVR-DA, and SVR-GWO, they were conducted using MATLAB environment.

III.2.3. Statistical evaluation

In evaluating our previous algorithms, SVR, SVR-PSO, SVR-DA, and SVR-GWO, four well-known statistical indicators were used to be able to measure the quality of the predictive ability of our algorithms and to be able to also compare with other works, including the coefficient of determination (R^2), root mean square error (RMSE), and the percent average absolute relative deviation (AARD%), are given by equations from (III.6) to (III.8):

$$R^2 = 1 - \left(\frac{\sum_{i=1}^{n}((Y - Y_{cal})^2)}{\sum_{i=1}^{n}((Y_{cal} - \bar{Y})^2)}\right) \quad \text{(III.6)}$$

$$RMSE = \sqrt{\frac{1}{n}\sum_{i=1}^{n}(Y_{cal} - Y)^2} \quad \text{(III.7)}$$

$$\text{AARD} = \frac{100}{n}\sum_{i=1}^{n}\left|\frac{Y_{cal} - Y}{Y}\right| \quad \text{(III.8)}$$

III.3. Results and Discussion

III.3.1. Effect of inputs on output

III.3.1.1. Relative importance of inputs

It can be defined as the effect of the inputs on the output for both models. For that, an approach developed by Üstün et al. [102] was followed which allowed the obtainment of the input's relative importance. It consists of using alpha values resulting from the Quadratic Programming (QP) with the reduced input data matrix (after removing the data that correspond to the zero alphas). An input profiling vector is obtained after the inner multiplication of the alpha vector and the reduced matrix. The profiling vector was then converted to percentages that sum up to 100%, to get a clear view of the evaluation.

We can see in the following two figures III.1 and III.2 the amount of importance of each input, and the type of its contribution, whether positive or negative, so that we are aware of which of them must be reduced and which of them must be increased to obtain a pressure drop in the range that achieves the best efficiency. Where, as we see in Figure III.1 the inputs with the greatest impact are fluid velocity and particle diameter with the highest positive impact, where, respectively, there is a relative relationship of 56.8% and 50.5%, meaning it is a direct relationship. Whenever we increase these inputs, we obtain a greater pressure drop. It is followed by the viscosity of the fluid, bed height, and porosity with a moderate effect and with a relative relationship of 27.7%, 25.5%, and 14.4%, respectively, and the density of the solid comes with a low effect, and with a relationship equal to 7%. On the other hand, the strongest negative effect is for Cos (α), then the inner diameter of the tube has a relationship of -48.2% and -29.5%

respectively, which indicates that as we increase these specifications, we get a lower pressure drop, and in the end the density of the fluid comes with the least negative effect, equal to -4.2%.

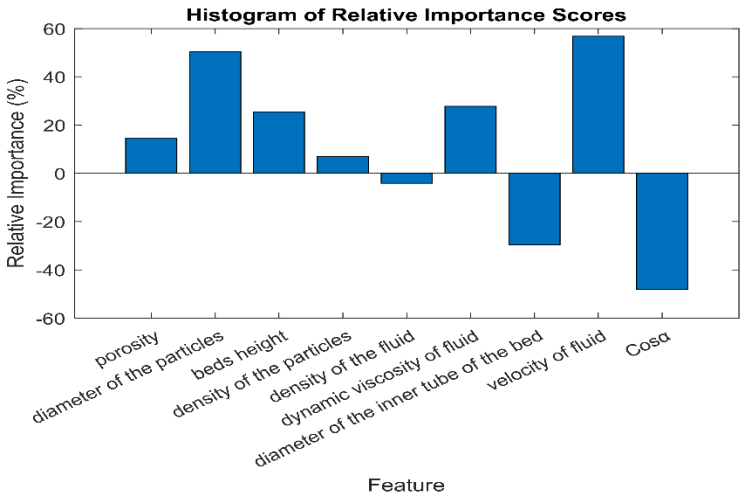


Figure III. 1. Histogram of inputs' relative importance (Normal model)

Figure III.2 shows the effect of the inputs in the second model on the Euler number, which is indicative of pressure drop, as we can see, the only input with a positive effect is the Reynolds number, which has a relative relationship of 68.5%, and as for the rest of the descriptors, they have a moderate negative effect. The Archimedes number is -32.5%, with a small effect of cos alpha, pipe inner diameter/bed height, and hydraulic diameter/particle diameter, with a relative relationship of -12.5%, -9.9%, and -3.5%, respectively.

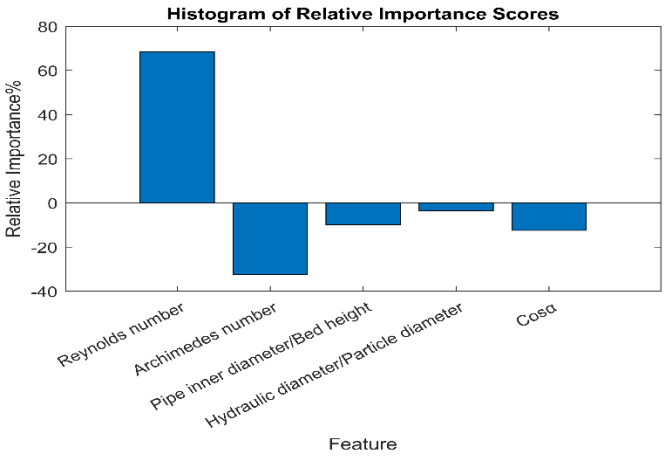


Figure III. 2. Histogram of inputs' relative importance (Dimensionless model)

III.3.1.2. Violin boxplot of the effect of inputs

Combining boxplots and kernel density charts, a violin plot illustrates numerical data. When working with multimodal data, it can be helpful to see the whole distribution of the data. Figure III.3 and III.4 show violin plots of the effect of inputs on output, whereas to read violin shapes, areas with a larger width indicate the density of the data range at that value.

It is possible to state that the distinction between violin charts showing the influence of inputs on output and the relative importance of inputs. Violin plots show how the output variable is distributed over various input categories, providing information on how inputs impact the distribution of the result. Conversely, relative significance analysis provides a numerical rating of the relevance of each input variable by quantifying its effect on the output's variability or prediction. Both methods offer distinct viewpoints and information kinds, but they are useful for comprehending the connection between inputs and results.

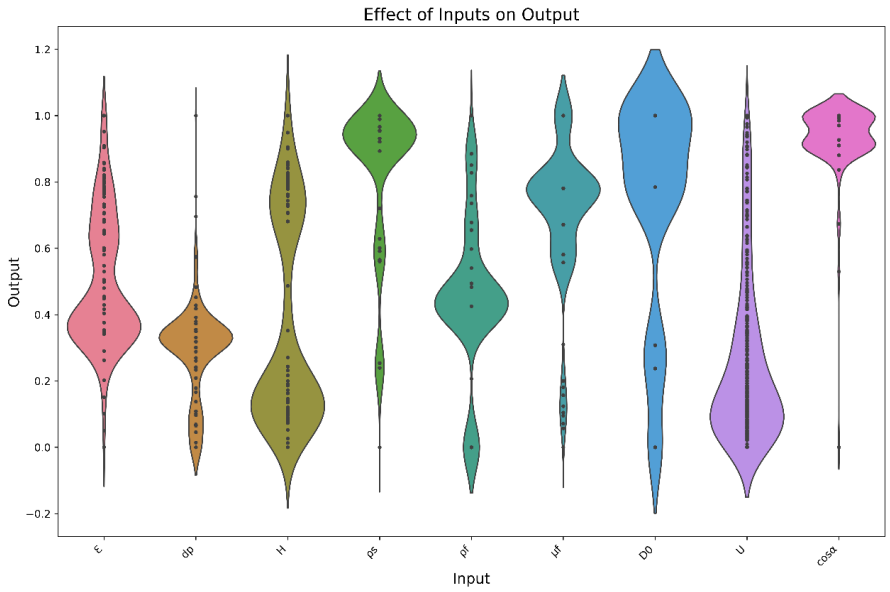


Figure III. 3. Violin plots of the effect of inputs on output (Normal model)

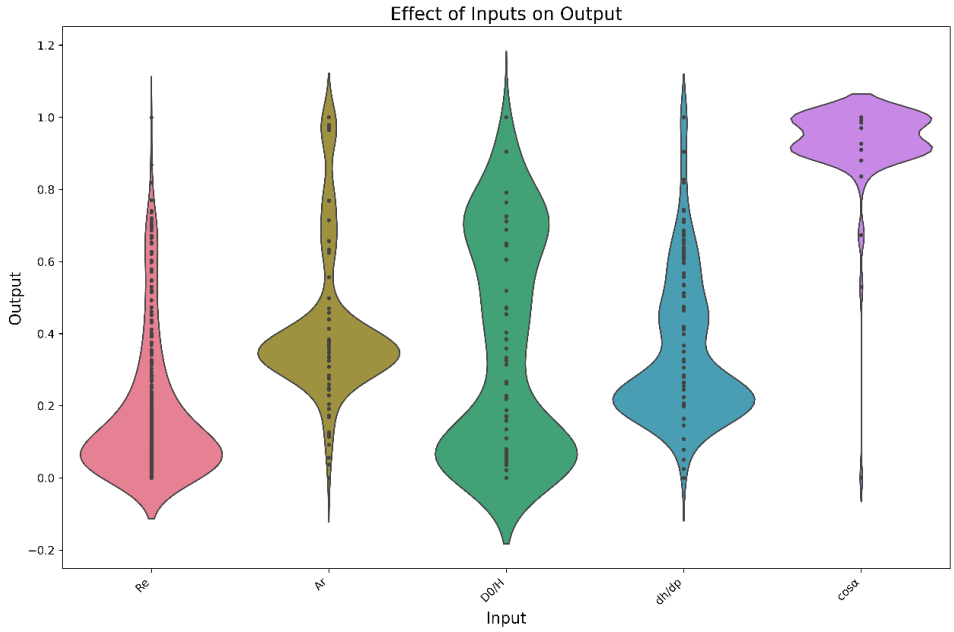


Figure III. 4. Violin plots of the effect of inputs on output (Dimensionless model)

III.3.2. SVR models development

III.3.2.1. Support vector regression model

(i) Normal model

In the present investigation, we conduct a thorough examination of Support Vector Regression (SVR), focusing on the determination of hyper-parameters and their impact on predictive accuracy. Our analysis is performed using the standard model framework, as specified in Table III.1. Through rigorous experimentation, we determined an optimal set of hyper-parameters characterized by C=1000, γ=10, ε=0.09, and the Radial Basis Function RBF as the kernel function. The results reveal significant findings, including coefficients of determination (R=0.9324, R^2=0.8484) and minimized error metrics (RMSE=0.1949, AARD=9.7106%). Additionally, the graphical representation in Figure III.5 elucidates the agreement between actual and predicted pressure drops across both training and testing datasets, providing a comprehensive comparison of the predictive capabilities of the SVR model.

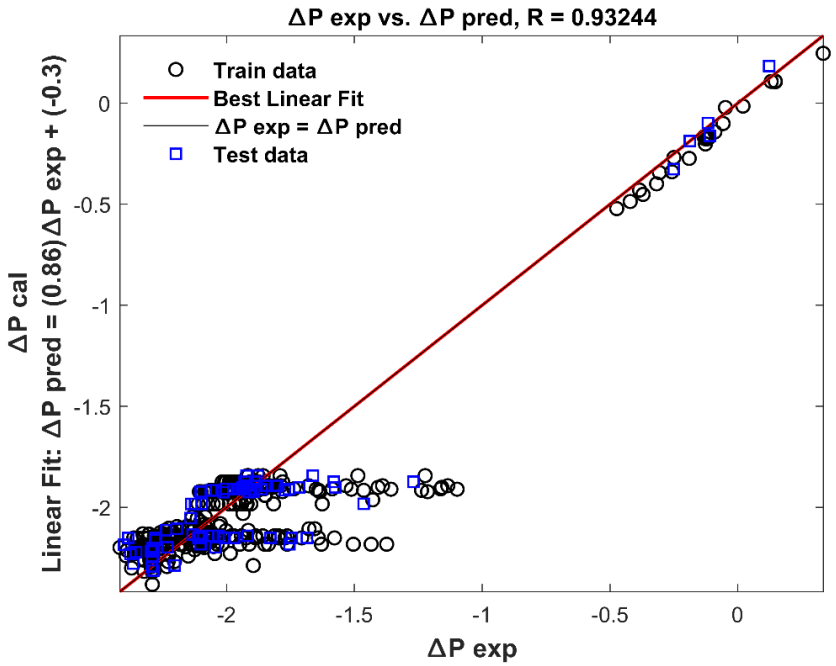


Figure III. 5. Actual versus the predicted pressure drop values by the SVR model

(ii)Dimensionless model

In the subsequent investigation, employing Support Vector Regression (SVR) within the dimensionless model framework as outlined in Table III.2, using the same last hyper-parameter C=1000, γ=10, ε= 0.09, and the Radial Basis Function RBF as the kernel function. The outcomes demonstrated coefficients of determination (R= 0.9821, R^2= 0.9628) along with a slight decrease in error metrics (RMSE=0.1659, AARD=7.1223 %). Notably, the graphical representation in Figure III.6 illustrates the correlation between actual and predicted Euler numbers for both training and testing datasets, providing a detailed comparison of the predictive performance of the SVR model.

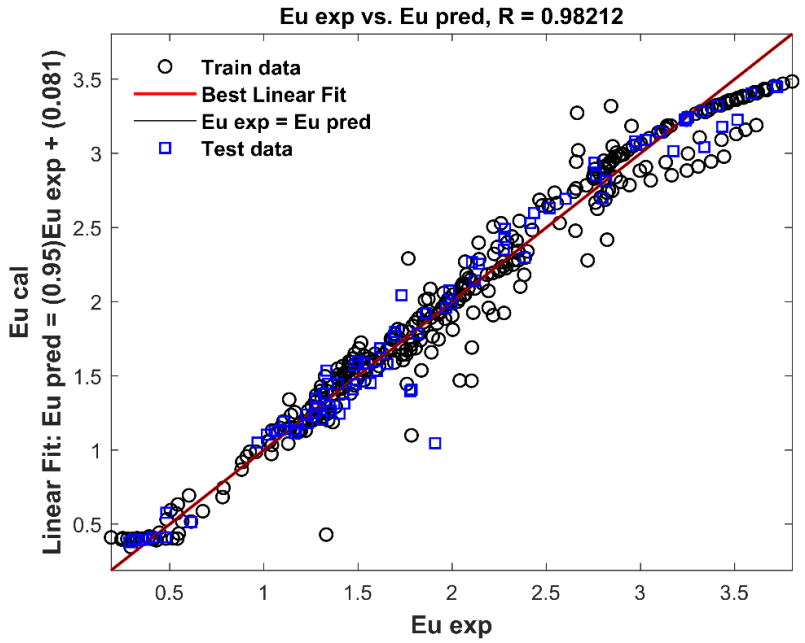


Figure III. 6. *Actual versus the predicted Euler number values by the SVR model*

III.3.2.2. SVR-dragonfly algorithm model

(i) Normal model

In the present investigation, we undertake an examination of a composite algorithm integrating Support Vector Regression (SVR) and Dragonfly Algorithm (DA), with the explicit objective of scrutinizing the ramifications of algorithmic adjustments on the selection of hyper-parameters. To accomplish that we conduct the examination in the normal model, delineated in Table III.1. The discernment of an optimal hyper-parameter configuration, characterized by C=125.504, γ=1.314, and ε=0.0461, ensued from our empirical inquiry. Noteworthy findings include elevated coefficients of determination (R=0.9840, R^2=0.9653), concomitant with minimized error metrics (RMSE=0.09632, AARD=5.4879%), denoting an enhanced predictive capacity. Additionally, the graphical exposition depicted in Figure III.7 elucidates the concordance between actual and predicted pressure drop across both training and testing partitions, affording a nuanced juxtaposition of predictive performance compared to the previous algorithmic framework paradigm.

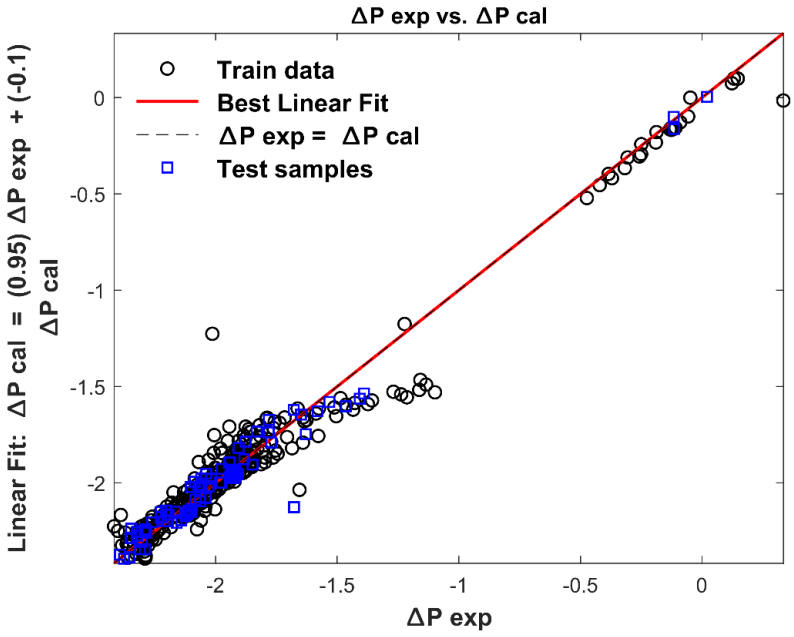


Figure III. 7. Actual versus the predicted pressure drop values by the SVR-DA model

(ii)Dimensionless model

In the subsequent investigation, employing the identical amalgamated algorithm featuring Support Vector Regression (SVR) and Dragonfly Algorithm (DA), using the dimensionless model, as detailed in Table III.2. The outcomes revealed a distinct set of optimal hyper-parameter values, specifically C=68.320, γ=0.8645, and ε =0.0639. This iteration yielded commendable coefficients of determination (R=0.99669, R^2=0.99322), accompanied by a modest increase in error metrics (RMSE=0.07223, AARD=1.1549%). Notably, Figure III.8 depicts the graphical representation of the correlation between actual and predicted Euler numbers across both training and testing datasets, affording a nuanced juxtaposition of predictive performance compared to the previous algorithmic framework paradigm.

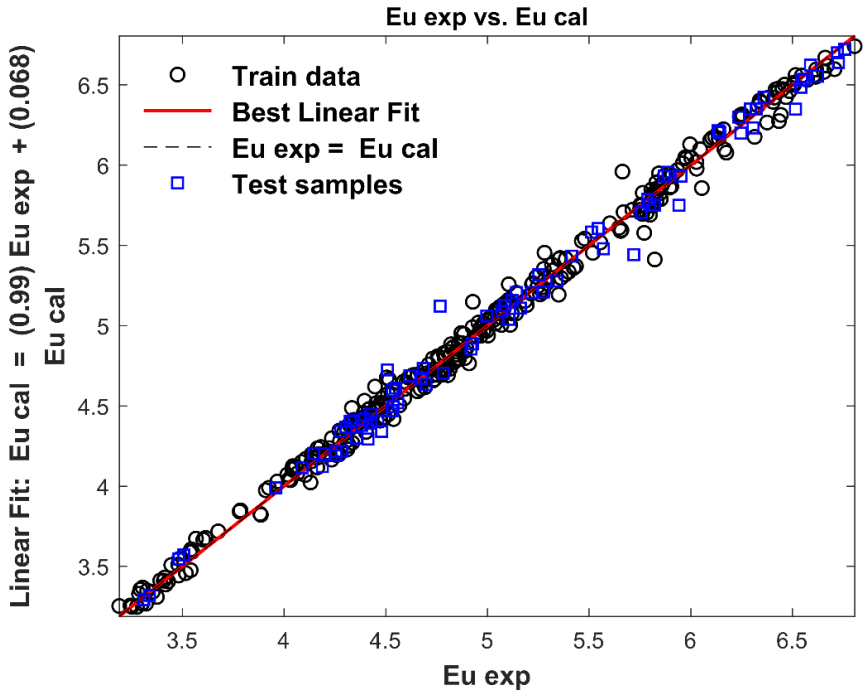


Figure III. 8. Actual versus the predicted Euler number values by the SVR-DA model

III.3.2.3. SVR- grey wolf optimizer model

(i) Normal model

Regarding the third algorithm, which integrates Support Vector Regression (SVR) with Grey Wolf Optimizer (GWO), subsequent to algorithm formulation and parameter calibration, it was implemented on the normal model delineated in Table III.1. The optimal combination of hyper-parameters yielded C=138.940, γ=0.3368, and ε=0.05114. Evaluation metrics manifested noteworthy performance: R=0.9485, R^2=0.8837, RMSE=0.17236, and AARD=3.17506%, signifying a commendable outcome. Additionally, Figure III.9 illustrates the correlation between observed and predicted pressure drop across training and testing datasets.

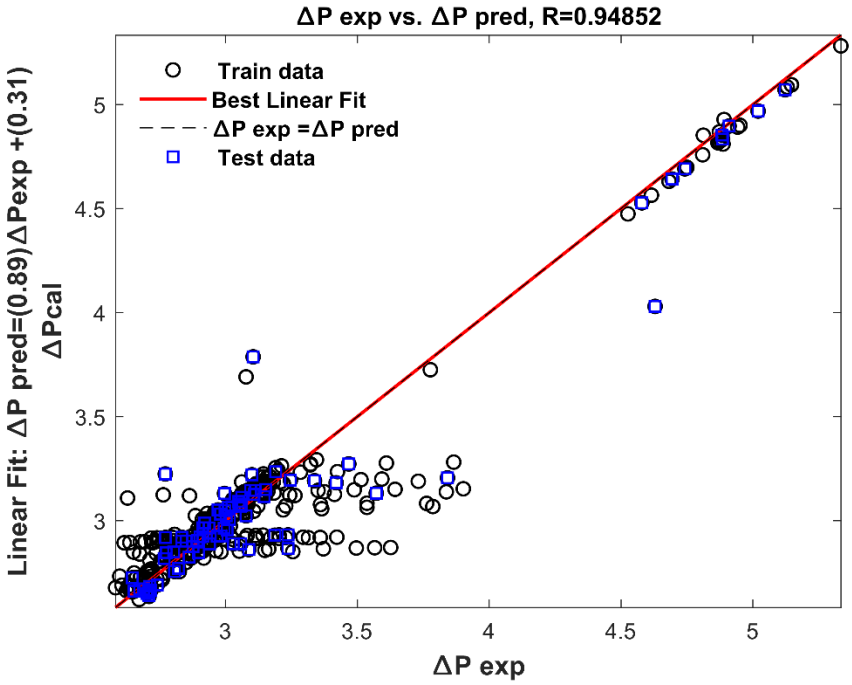


Figure III. 9. Actual versus the predicted pressure drop values by the SVR-GWO

(ii)Dimensionless model

Upon subjecting our dimensionless model, delineated in Table III.2, to the same amalgamation of SVR and GWO algorithm, the optimal hyper-parameter configuration was determined: C=144.7099, γ=2.8794, and ε=0.08130. The evaluation metrics reflected notable performance: R=0.99252, R^2=0.98472, RMSE=0.1085, and AARD=1.5528%. Furthermore, Figure III.10 illustrates the relationship curve between observed and predicted Euler numbers across training and testing datasets.

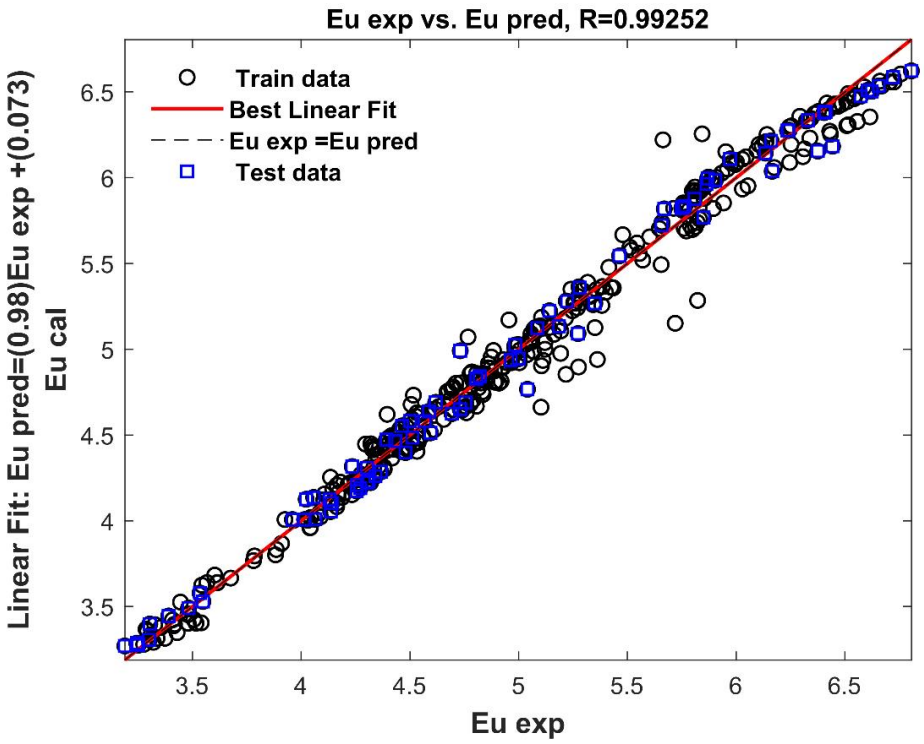


Figure III. 10. Actual versus the predicted Euler number values by the SVR-GWO

III.3.2.4. SVR- particle swarm optimization model

(i) Normal model:

The fourth algorithm come from the integration of Support Vector Regression (SVR) and Particle Swarm Optimization (PSO) methodologies, aimed at optimizing hyper-parameter selection. This novel approach was employed to minimize error values by conducting extensive testing within the specified domain, consistent with our methodology in previous algorithms. Application of this algorithm to a normal model, detailed in Table III.1, yielded optimal parameter values: C=500, γ=6.5627, and ε=0.0208. This parameterization effectively mitigated overfitting concerns, resulting in improved performance metrics, as evidenced by a higher coefficient of determination (R^2=0.98179), a robust correlation coefficient (R=0.99138), and reduced root mean square error (RMSE=0.0708) and average absolute relative deviation (AARD=1.4299%). Notably, these outcomes surpass prevailing benchmarks in the literature, affirming the efficacy of our approach. Additionally, Figure III.11 depicts the relationship between actual and predicted pressure drop across training and test datasets.

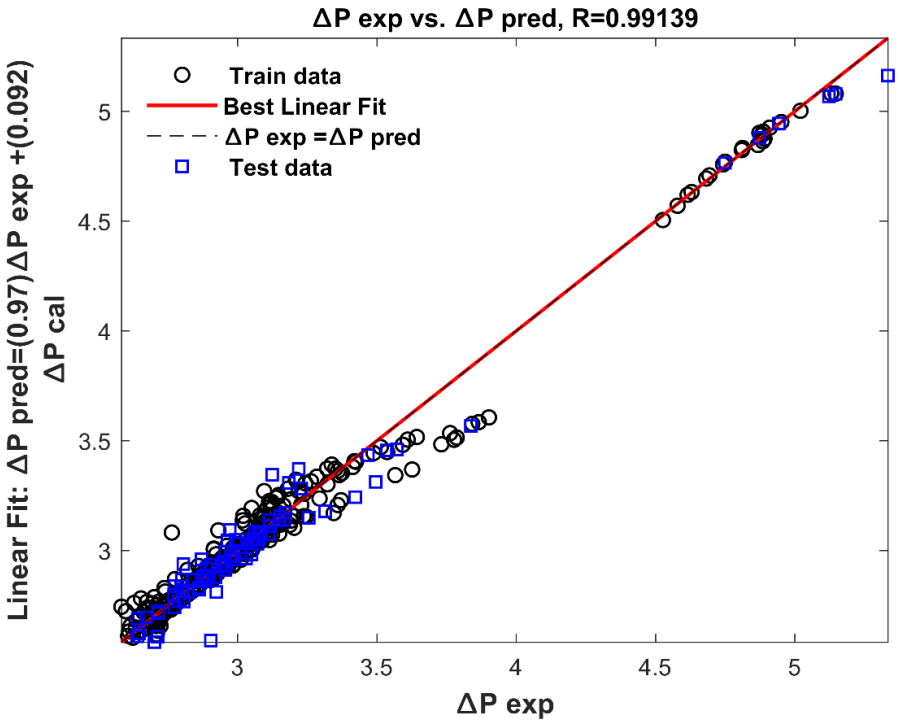


Figure III. 11. Actual versus the predicted pressure drop values by the SVR-PSO model

(ii) dimensionless model

Following experimentation, the combination of the PSO and SVR algorithm was applied to a dimensionless model, as outlined in Table III.2. The resultant hyper-parameters were determined to be C=218.410, γ=1, and ε=0.00434. Comparative analysis revealed superior performance metrics relative. Specifically, a high correlation coefficient (R=0.99858) and coefficient of determination (R^2=0.99715) were achieved, root mean square error (RMSE=0.0472) and average absolute relative deviation (AARD=0.5235%). Remarkably, these advancements were attained utilizing an equivalent quantity of vectors. Thus, our utilization of the dimensionless model has yielded notable improvements, surpassing the accuracy of the conventional model. Additionally, Figure III.12 visually illustrates the relationship between actual and predicted Euler numbers across training and test datasets.

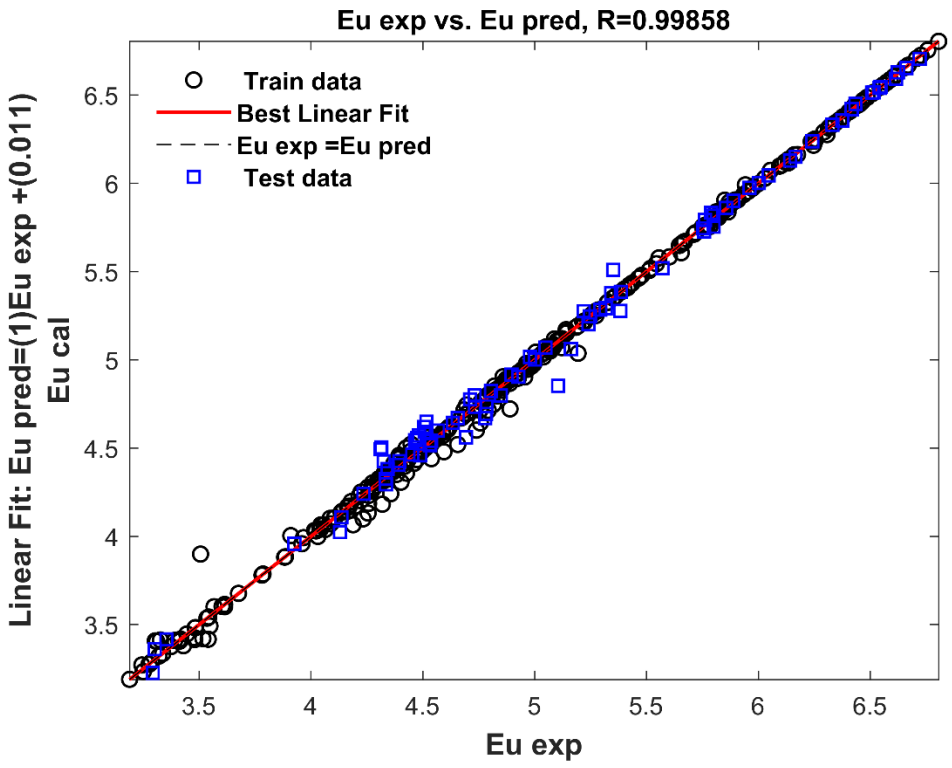


Figure III. 12. Actual versus the predicted Euler number values by the SVR-PSO

III.3.2.5. External validation

External validation was performed using the external validation tool downloaded from (https://sites.google.com/site/dtclabxvplus/), which contains the tool and a full explanation of its use.

After looking at Table III.3, which reviews the results of the external validation of the models and algorithms that we worked on, the table shows that most of the algorithms, in varying proportions, provided excellent performance, with the exception of the SVR normal model (N), which provided somewhat poor performance, as shown by the CCC and the value of the high root mean square error RMSE where the values range down. The SVR-PSO dimensionless model (D), showed the best results with regard to high CCC and Q^2 values, and lower RMSE, which indicates good statistical significance and high robustness.

- CCC (Concordance Correlation Coefficient)

CCC takes precision and accuracy into account when assessing the degree of agreement between anticipated and observed values. The model's precision and dependability are highlighted

by the global CCC of 0.9408, which shows a high degree of agreement between the model's predictions and experimental results.

- Q^2 (Cross-validation coefficient)

One crucial parameter in cross-validation is Q^2, which indicates the model's ability to predict novel, unobserved data points. The robustness of the model is demonstrated by a global Q^2 of 0.8511, implying that it can explain approximately 85.11% of the variance in new data. Essentially, Q^2 assesses the model's generalization capability beyond the training set. As evidenced by the results, a Q^2 value exceeding 0.5 signifies that the model is proficient in generating reliable predictions for new observations.

Table III. 3. External validation criteria for all models

Model	Validation criteria			
	R^2	RMSE	CCC	Q^2
SVR(N)	0.873	0.1949	0.9295	0.9986
SVR(D)	0.9654	0.1659	0.9819	0.9897
SVR-DA (N)	0.9683	0.0963	0.9833	0.9997
SVR-DA (D)	0.9934	0.0722	0.9966	0.9985
SVR-GWO (N)	0.8997	0.1724	0.9454	0.9174
SVR-GWO (D)	0.9851	0.1085	0.9924	0.9966
SVR-PSO (N)	0.9829	0.0708	0.9911	0.9861
SVR-PSO (D)	0.9972	0.0472	0.9986	0.9994

III.3.2.6. General comparisons

(i) Dataset comparison: The findings reveal that among the four algorithms evaluated, the dimensionless model exhibited superior performance compared to the normal model. This superiority is evidenced by the normal model achieving lower values for both RMSE and AARD, indicating enhanced predictive accuracy, alongside high R^2 values, signifying a greater proportion of variance explained within the variables. Consequently, the results underscore the distinct superiority of the dimensionless model, highlighting its quality and robustness.

(ii) Algorithms comparison: When comparing the four algorithms, the SVR-PSO algorithm consistently outperformed the others in all cases, followed by SVR-DA, SVR-GWO, and SVR

respectively. With SVR-PSO achieving the highest R^2 and the lowest RMSE and AARD values. The other algorithms were ranked accordingly. Notably, the Superiority of the three meta-heuristic optimization algorithms towards the SVR algorithm underscores the significant role of meta-heuristic optimization techniques. These performance differences are attributable to the distinct mechanisms underlying each algorithm's operation. Overall, the results consistently identified SVR-PSO, along with the dimensionless model, as the most effective among the algorithms evaluated.

(iii) Kernel density estimation plot comparisons: To make a comparison between the work of different algorithms using Kernel Density Estimation (KDE), we collected the actual test samples with the predicted ones for all the experiments that we conducted and subtracted them from each other to obtain the residual for each model. Then we represented the residual for the dimensionless model in the y-axis and the residual for the normal model in the x-axis, and the representation was performed by the KDE process, they were conducted using Python codes.

The KDE method works by representing points graphically, which in our case is close to zero for most points because it is the remainder of subtracting the actual value from the predicted value. Then it places a kernel (Gaussian in our case) on each data point, and then (sns.kdeplot) is used to estimate the density of points in our two-dimensional space, then comes the role of the color map (cmap) parameter, which assigns a specific color to each specific density value and changes the colors gradually as the density decreases, which is represented digitally in the sidebar so that the density value is shown with the corresponding color, where the other number indicates values. The point density is lower at that point and the larger number has higher density values, so as a summary, we can theoretically determine the density values for each point of color in the two-dimensional space in a smooth and professional way.

Where, as we see in figures from figure III.13 to III.16, which show the KDE plot diagram for all algorithms that are consistent with what we mentioned previously, we see in the figure for SVR-PSO the largest point density that approaches zero for the two axes and scales according to the algorithm used, and as we mentioned previously.

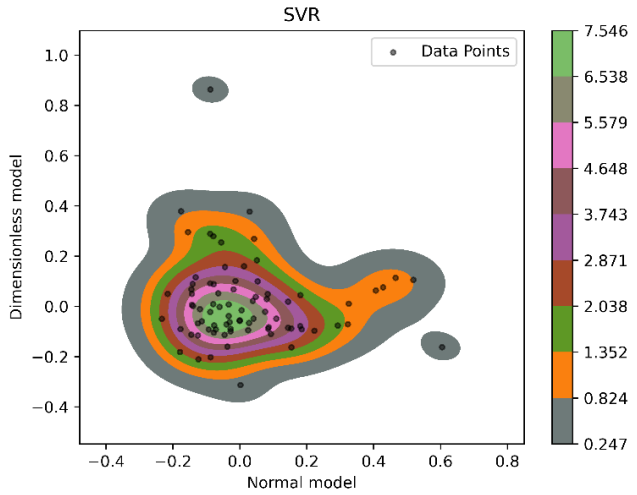


Figure III. 13. Kernel density estimation plot for SVR model

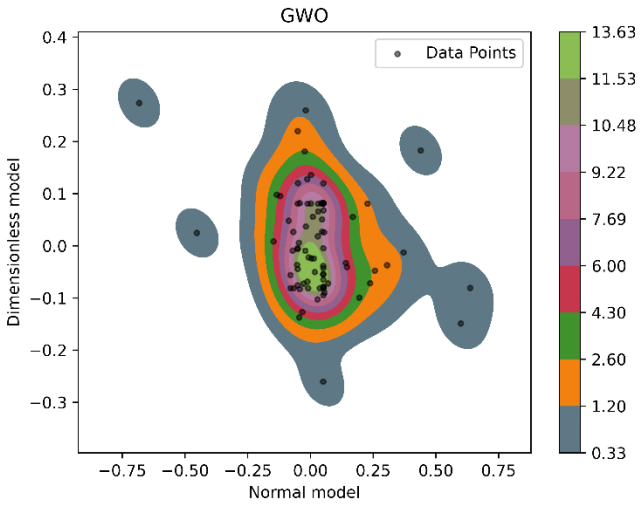


Figure III. 14. Kernel density estimation plot for SVR-GWO model

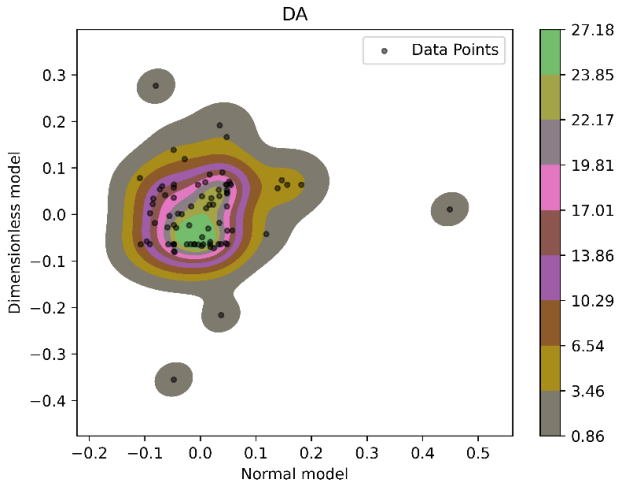


Figure III. 15. Kernel density estimation plot for SVR-DA model

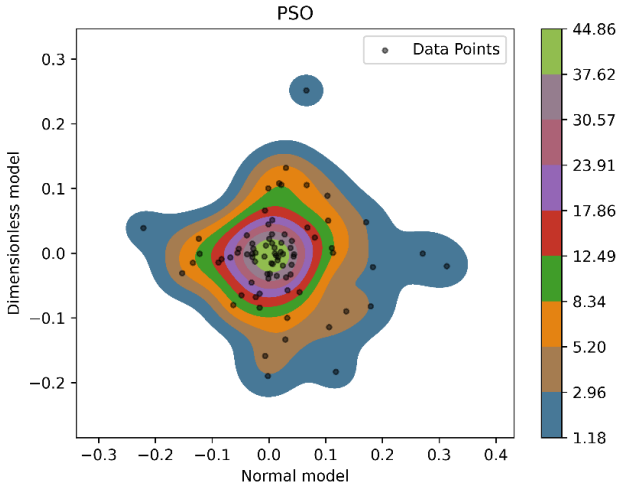


Figure III. 16. Kernel density estimation plot for SVR-PSO model

(iv) Correlation plot comparisons: As we can see in Figure III.17 and III.18, which indicate the correlations between the inputs in both of our models, show the Pearson correlation coefficient (R), whose range is between 1 and -1, which indicates that the correlation between the inputs is negative or positive, as it when it is positive, it indicates that when one of the inputs increases, it affects the other by increasing, and vice versa, when it is negative, and when its value is equal to zero, it indicates that there is no relationship between the inputs, which is usually used to determine multicollinearity, which occurs when there is a high correlation between the descriptors. As we notice in the figure for the dimensionless model, there is a decrease in the value of R compared to the regular model, which is one of the advantages of using it, as it is most suitable for overcoming the problem of multiple linear relationships.

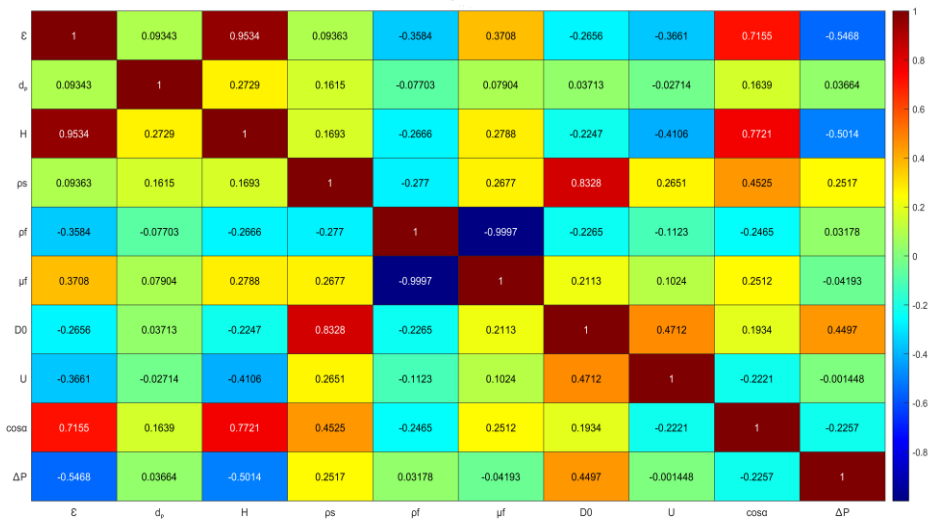


Figure III. 17. Correlation plot between inputs and output (Normal model)

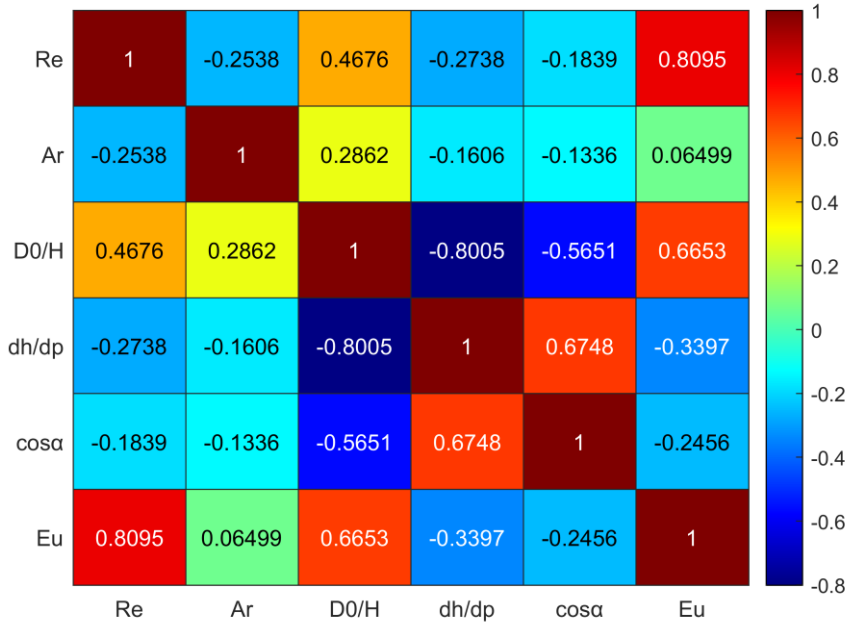
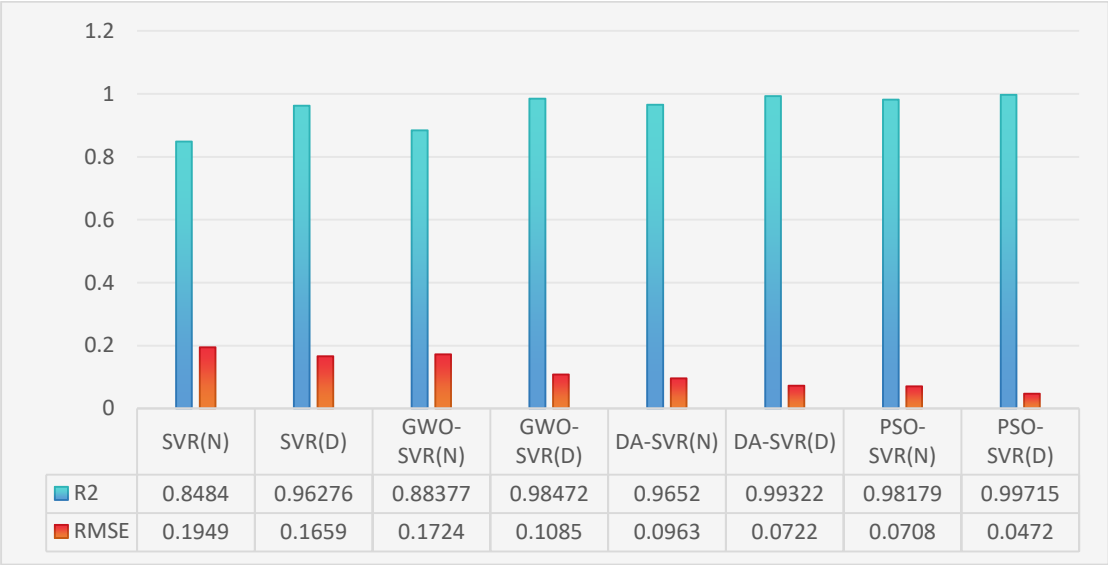


Figure III. 18. Correlation plot between inputs and output (Dimensionless model)

In Figure III.19, we see a graphical representation of both R^2 and RMSE obtained in our previous experiments, and in Figure III.20, we see a three-dimensional graphical representation of the number of AARDs within different ranges.



	SVR(N)	SVR(D)	GWO-SVR(N)	GWO-SVR(D)	DA-SVR(N)	DA-SVR(D)	PSO-SVR(N)	PSO-SVR(D)
R2	0.8484	0.96276	0.88377	0.98472	0.9652	0.99322	0.98179	0.99715
RMSE	0.1949	0.1659	0.1724	0.1085	0.0963	0.0722	0.0708	0.0472

Figure III. 19. Chart column of R^2 and RMSE for all models

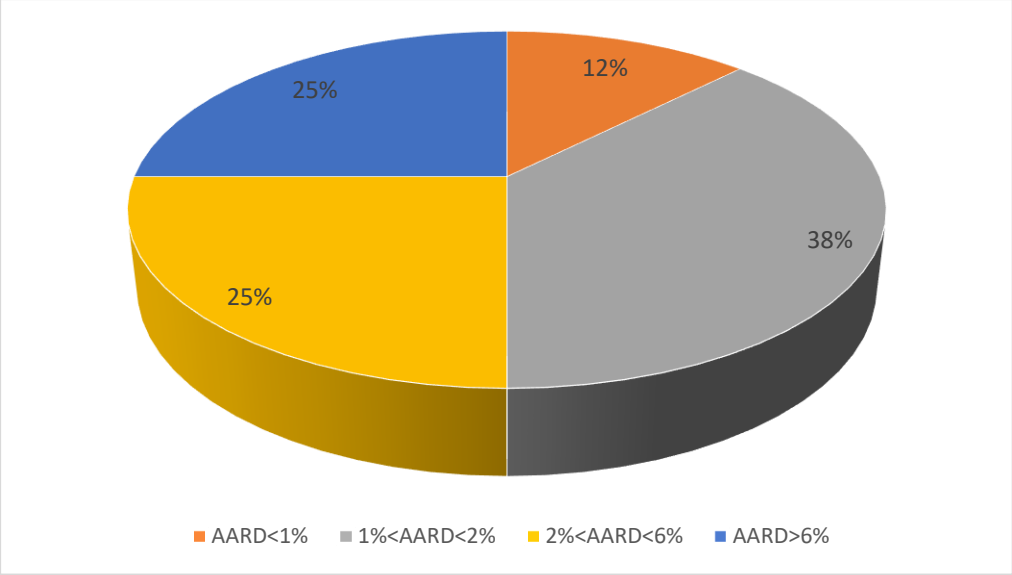


Figure III. 20. 3D pie for the number of Average absolute relative deviation (AARD) for different ranges

III.4. Conclusion

In this chapter, we were able to prove the effectiveness of using our various algorithms to obtain an accurate prediction of the pressure drop in the fluidized bed, with the SVR-PSO algorithm outperforming the rest of the algorithms.

We were able to prove the feasibility of the dimensionless system from more than one aspect, as the accuracy is superior to the regular model, and as we saw in the figures for the correlations between inputs and outputs, the clear decrease in correlations in the dimensionless model, which avoids many problems, as we mentioned previously.

We were able to review more of the impact that the inputs play on the outputs in more than one way to simplify the presentation and to enable us to obtain the greatest understanding of the phenomenon of pressure beds in the fluidized bed and the role that each element plays in it.

General conclusion

General Conclusion

In the realm of scientific research, particularly within the domain of fluidization and pressure drop in fluidized beds, this thesis represents a significant and groundbreaking contribution. It serves as a unique reference and guide for predicting pressure drop in cylindrical and conical fluidized beds through the application of artificial intelligence techniques, with a particular focus on Support Vector Machine (SVM) algorithms. As delineated in our thesis, measuring pressure in a fluidized bed is a complex task requiring the calibration of numerous parameters to achieve accurate results, notwithstanding the inherent risks of experimental failure.

To address these challenges, we established two primary objectives. The first objective was to achieve highly accurate predictions of pressure drop in cylindrical and conical fluidized beds using support vector machine algorithms, in light of the lack of previous research in this specific area. The second objective, equally important and complex, was to develop and validate the efficiency of a novel dimensionless system. This system aims to serve as an alternative to conventional systems, thereby mitigating persistent issues related to unit conversions that affect both students and educators. This new system is designed to be universal and applicable in various contexts, thereby resolving several problems, such as the correlations between inputs that researchers encounter when utilizing standard databases.

Finally, as a summary of all that has been said, our work is considered a precedent of its kind and a great and important addition to the world of liquefaction, which is widely used and widely spread in various industrial circles all over the world. We can summarize the most important results we have reached as follows:

-We were able to build and prove the high efficiency of a dimensionless model that can be used as an alternative to regular models that use units;

-We set a scientific precedent in the field of predicting pressure drop using support vector machine algorithms, which is work that no one has ever done before, and not only that but also using four different algorithms;

- The best and most accurate model was obtained using the SVR-PSO algorithm, making it the first in our database for two models dimensionless model and the normal model with the results and respectively (R^2=0.997, RMSE=0.047) and (R^2=0.982, RMSE=0.071);

- In our work, the weakest results were for the SVR algorithm, with the results for the two dimensionless and normal models and respectively (R^2=0.968, RMSE=0.166) and (R^2=0.848, RMSE=0.195) which is accepted in scientific circles;

-We proved the great importance of using meta-optimization algorithms after seeing the difference in results with and without using them;

-We can save a great deal of money, time and human energies when using artificial intelligence as an alternative to conducting practical experiments, especially after the highly accurate and impressive results that we saw in our study;

- Opening the door to the possibility of trying other meta-optimization algorithms such as BA, ABC;

- Opening horizons to reconsider the system of units used globally;

-The use of Python codes allowed the results to be presented in a professional manner that combines simplicity in presentation and ease of understanding, as we saw in the KDE forms.

[1] Y. Lv, F. Hong, T. Yang, F. Fang, and J. Liu, "A dynamic model for the bed temperature prediction of circulating fluidized bed boilers based on least squares support vector machine with real operational data," *Energy*, vol. 124, pp. 284–294, Apr. 2017, doi: 10.1016/j.energy.2017.02.031.

[2] Y. Lv, J. Liu, and T. Yang, "Nonlinear PLS Integrated with Error-Based LSSVM and Its Application to NO x Modeling," Ind. Eng. Chem. Res., vol. 51, no. 49, pp. 16092–16100, Dec. 2012, doi: 10.1021/ie3005379.

[3] P. Kadlec, B. Gabrys, and S. Strandt, "Data-driven Soft Sensors in the process industry," Comput. Chem. Eng., vol. 33, no. 4, pp. 795–814, Apr. 2009, doi: 10.1016/j.compchemeng.2008.12.012.

[4] Y. Lv, T. Yang, and J. Liu, "An adaptive least squares support vector machine model with a novel update for NOx emission prediction," Chemom. Intell. Lab. Syst., vol. 145, pp. 103–113, Jul. 2015, doi: 10.1016/j.chemolab.2015.04.006.

[5] R. Grbić, D. Slišković, and P. Kadlec, "Adaptive soft sensor for online prediction and process monitoring based on a mixture of Gaussian process models," Comput. Chem. Eng., vol. 58, pp. 84–97, Nov. 2013, doi: 10.1016/j.compchemeng.2013.06.014.

[6] C. G. Hill and T. W. Root, Introduction to chemical engineering kinetics and reactor design. John Wiley & Sons, 2014.

[7] P. Glavič, "Quantities and Units in Chemical and Environmental Engineering," Standards, vol. 2, no. 1, pp. 43–51, Feb. 2022, doi: 10.3390/standards2010004.

[8] N. N. Loginov and A. M. Nizovtsev, "Application of the international system of units in Chemical Engineering," Meas. Tech., vol. 10, no. 12, pp. 1532–1534, Dec. 1967, doi: 10.1007/BF00981298.

[9] M. J. Rhodes, Introduction to particle technology. John Wiley & Sons, 2008.

[10] M. Rasteh, F. Farhadi, and A. Bahramian, "Hydrodynamic characteristics of gas–solid tapered fluidized beds: Experimental studies and empirical models," Powder Technol., vol. 283, pp. 355–367, Oct. 2015, doi: 10.1016/j.powtec.2015.06.002.

[11] R. S. Subramanian, "Flow through Packed and Fluidized Beds," Dep. Chem. Biomol. Eng. Clarkson Univ. Potsdam NY USA, 2002.

[12] R. Cocco, S. B. R. Karri, and T. Knowlton, "Introduction to Fluidization," Back Basics, 2014.

[13] S. Fang, Y. Wei, L. Fu, G. Tian, and H. Qu, "Modeling of the Minimum Fluidization Velocity and the Incipient Fluidization Pressure Drop in a Conical Fluidized Bed with Negative Pressure," Appl. Sci., vol. 10, no. 24, p. 8764, Dec. 2020, doi: 10.3390/app10248764.

[14] A. Madani, O. Benkortbi, and M. Laidi, "In silico prediction of the inhibition of new molecules on SARS-CoV-2 3CL protease by using QSAR: PSOSVR approach," Braz. J. Chem. Eng., vol. 41, no. 1, pp. 427–442, Mar. 2024, doi: 10.1007/s43153-023-00332-z.

[15] Y. Yan, T. N. Borhani, and P. T. Clough, "Machine Learning Applications in Chemical Engineering," in Machine Learning in Chemistry, H. M. Cartwright, Ed., The Royal Society of Chemistry, 2020, pp. 340–371. doi: 10.1039/9781839160233-00340.

[16] Y. Ren and G. Bai, "Determination of optimal SVM parameters by using GA/PSO.," J Comput, vol. 5, no. 8, pp. 1160–1168, 2010.

[17] C. Li, X. An, and R. Li, "A chaos embedded GSA-SVM hybrid system for classification," Neural Comput. Appl., vol. 26, no. 3, pp. 713–721, Apr. 2015, doi: 10.1007/s00521-014-1757-z.

[18] Q. Shen, J.-H. Jiang, C.-X. Jiao, G. Shen, and R.-Q. Yu, "Modified particle swarm optimization algorithm for variable selection in MLR and PLS modeling: QSAR studies of antagonism of angiotensin II antagonists," Eur. J. Pharm. Sci., vol. 22, no. 2–3, pp. 145–152, Jun. 2004, doi: 10.1016/j.ejps.2004.03.002.

[19] P. Shelokar, A. Kulkarni, V. K. Jayaraman, and P. Siarry, "Metaheuristics in Process Engineering: A Historical Perspective," in Applications of Metaheuristics in Process Engineering, J. Valadi and P. Siarry, Eds., Cham: Springer International Publishing, 2014, pp. 1–38. doi: 10.1007/978-3-319-06508-3_1.

[20] Y. R. Nugraha, A. P. Wibawa, and I. A. E. Zaeni, "Particle Swarm Optimization – Support Vector Machine (PSO-SVM) Algorithm for Journal Rank Classification," in 2019 2nd International Conference of Computer and Informatics Engineering (IC2IE), Banyuwangi, Indonesia: IEEE, Sep. 2019, pp. 69–73. doi: 10.1109/IC2IE47452.2019.8940822.

[21] Y. Liang, S. Hu, W. Guo, and H. Tang, "Abrasive tool wear prediction based on an improved hybrid difference grey wolf algorithm for optimizing SVM," Measurement, vol. 187, p. 110247, Jan. 2022, doi: 10.1016/j.measurement.2021.110247.

[22] M. Alshinwan et al., "Dragonfly algorithm: a comprehensive survey of its results, variants, and applications," Multimed. Tools Appl., vol. 80, no. 10, pp. 14979–15016, Apr. 2021, doi: 10.1007/s11042-020-10255-3.

[23] M. Horio, "Fluidization science, its development and future," Particuology, vol. 8, no. 6, pp. 514–524, Dec. 2010, doi: 10.1016/j.partic.2010.08.010.

[24] https://www.kkt-chillersusa.com/understanding-pressure-drop-and-its-impact-on-your- processing-system/

[25] https://klarenbv.com/fluidization/

[26] https://www.merriam-webster.com/dictionary/fluidize

[27] D. Kunii and O. Levenspiel, Fluidization engineering. Butterworth-Heinemann, 1991.

[28] https://blog.iqsdirectory.com/fluid-bed-dryers-3/

[29] https://msubbu.in/ln/fm/Unit-IV/Fluidization.htm

[30] T. M. Knowlton, D. L. Keairns, and W.-C. Yang, "History of fluidization in North America," Powder Technol., vol. 426, p. 118609, Aug. 2023, doi: 10.1016/j.powtec.2023.118609.

[31] B. Leckner, "Developments in fluidized bed conversion of solid fuels," Therm. Sci., vol. 20, no. suppl. 1, pp. 1–18, 2016, doi: 10.2298/TSCI150703135L.

[32] D. Kunii and O. Levenspiel, "Circulating fluidized-bed reactors," Chem. Eng. Sci., vol. 52, no. 15, pp. 2471–2482, Aug. 1997, doi: 10.1016/S0009-2509(97)00066-3.

[33] W. Lewis, "Entrainment of solids from fluidized beds," 1953.

[34] J. J. Barker, "HEAT TRANSFERICIENTS IN FLUIDIZED BEDS," Ind. Eng. Chem., vol. 57, no. 5, pp. 33–39, May 1965, doi: 10.1021/ie50665a007.

[35] https://www.researchgate.net/post/What_is_the_range_of_pressure_drop_across_the_ air_distributor_in_fluidization_of_particles

[36] B. Halvorsen and B. Arvoh, "Minimum fluidization velocity, bubble behaviour and pressure drop in fluidized beds with a range of particle sizes," WIT Trans. Eng. Sci., vol. 63, pp. 227–238, 2009.

[37] E. S. Qassem, S. H. Mohammed, and T. N. Sarmad, "Effect of fluidization on pressure drop and power consumption in packed bed columns," IOP Conf. Ser. Mater. Sci. Eng., vol. 671, no. 1, p. 012070, Jan. 2020, doi: 10.1088/1757-899X/671/1/012070.

[38] J. B. Drake, Hydrodynamic characterization of 3D fluidized beds using noninvasive techniques. Iowa State University, 2011.

[39] A. Rao, J. S. Curtis, B. C. Hancock, and C. Wassgren, "The effect of column diameter and bed height on minimum fluidization velocity," AIChE J., vol. 56, no. 9, pp. 2304–2311, Sep. 2010, doi: 10.1002/aic.12161.

[40] F. Villers, "Bed porosity in a magnetically stabilized liquid-solid fluidized bed," 1998.

[41] https://www.drillingformulas.com/what-is-porosity/

[42] H. Ridha and M. G. Al-Azawy, "Study of the effect of particle diameters on two-phase (air-solid) fluidization bed hydrodynamics," Mater. Today Proc., vol. 42, pp. 2113–2118, 2021, doi: 10.1016/j.matpr.2020.12.294.

[43] R. Timsina, R. K. Thapa, B. M. E. Moldestad, and M. S. Eikeland, "Effect of particle size on flow behavior in fluidized beds," Int. J. Energy Prod. Manag., vol. 4, no. 4, pp. 287–297, Nov. 2019, doi: 10.2495/EQ-V4-N4-287-297.

[44] Y. Wang, T. Lu, and K. Wang, "Effect of particle diameter of porous media on flow and heat transfer in a mixing tee," Ann. Nucl. Energy, vol. 49, pp. 122–130, Nov. 2012, doi: 10.1016/j.anucene.2012.05.031.

[45] J. Peng, W. Sun, L. Xie, H. Han, and Y. Xiao, "An Experimental Study of Pressure Drop Characteristics and Flow Resistance Coefficient in a Fluidized Bed for Coal Particle Fluidization," Minerals, vol. 12, no. 3, p. 289, Feb. 2022, doi: 10.3390/min12030289.

[46] H. Upender and K. A. Kishore, "Effect of temperature and apparent liquid viscosity on the hydrodynamics of liquid–solid tapered inverse fluidized bed: experimental studies compared with empirical models," SN Appl. Sci., vol. 2, no. 4, p. 622, Apr. 2020, doi: 10.1007/s42452-020-2365-4.

[47] J. Aronsson, D. Pallarès, M. Rydén, and A. Lyngfelt, "Increasing Gas–Solids Mass Transfer in Fluidized Beds by Application of Confined Fluidization—A Feasibility Study," Appl. Sci., vol. 9, no. 4, p. 634, Feb. 2019, doi: 10.3390/app9040634.

[48] H. Altzibar, G. Lopez, J. Bilbao, and M. Olazar, "Effect of draft tube geometry on pressure drop in draft tube conical spouted beds," Can. J. Chem. Eng., vol. 91, no. 11, pp. 1865–1870, Nov. 2013, doi: 10.1002/cjce.21913.

[49] M. Khani, "Models for prediction of hydrodynamic characteristics of gas–solid tapered and mini-tapered fluidized beds," Powder Technol., vol. 205, no. 1–3, pp. 224–230, 2011.

[50] B. Pelikan, The Pump Book. Lulu. com, 2007.

[51] https://physics.stackexchange.com/questions/461861/does-pressure-decreases-in-accelerating-fluids

[52] L. Liao, "Influence of particle shape and bed height on fluidization," 2013.

[53] J. R. van Ommen and R. F. Mudde, "Measuring the Gas-Solids Distribution in Fluidized Beds--A Review," Int. J. Chem. React. Eng., vol. 6, no. 1, 2008.

[54] https://forum.arduino.cc/t/pressure-sensor-choice-for-fluidized-bed/194499

[55] A. A. Abdulrahman et al., "Experimental Investigation and Computational Fluid Dynamic Simulation of Hydrodynamics of Liquid–Solid Fluidized Beds," ChemEngineering, vol. 6, no. 3, p. 37, May 2022, doi: 10.3390/chemengineering6030037.

[56] R. Turton, R. C. Bailie, W. B. Whiting, and J. A. Shaeiwitz, Analysis, synthesis and design of chemical processes. Pearson Education, 2008.

[57] https://blog.dwyer-inst.com/2018/08/01/air-velocity-and-flow-measurement-with-pitot-tubes-2/#sthash.Z6kDFYJj.dpbs

[58] W. L. Cook, An experimental apparatus for measurement of pressure drop, void fraction, and non-boiling two-phase heat transfer and flow visualization in pipes for all inclinations. Oklahoma State University, 2008.

[59] P. S. Pillay and Y. B. G. Varma, “Pressure drop and solids holding time in multistage fluidisation,” Powder Technol., vol. 35, no. 2, pp. 223–231, Jul. 1983, doi: 10.1016/0032-5910(83)87012-0.

[60] D. P. Chakrabarti, G. Das, and S. Ray, “Pressure Drop in Liquid-liquid Two Phase Horizontal Flow: Experiment and Prediction,” Chem. Eng. Technol., vol. 28, no. 9, pp. 1003–1009, Sep. 2005, doi: 10.1002/ceat.200500143.

[61] K. Hashizume, S. Morita, Y. Nakamura, and A. Wada, “Pressure Drop in Liquid-Solid Circulating Fluidized Beds,” Trans. Jpn. Soc. Mech. Eng. Ser. B, vol. 74, no. 743, pp. 1617–1624, 2008, doi: 10.1299/kikaib.74.1617.

[62] K. Hashizume, S. Morita, Y. Nakamura, and A. Wada, “Pressure drop in liquid–solid circulating fluidized beds,” Heat Transfer—Asian Res., vol. 38, no. 4, pp. 248–261, Jun. 2009, doi: 10.1002/htj.20241.

[63] A. Zakeri, A. Einbu, and H. F. Svendsen, “Experimental investigation of pressure drop in structured packings,” Chem. Eng. Sci., vol. 73, pp. 285–298, May 2012, doi: 10.1016/j.ces.2012.01.025.

[64] M. Mac Giolla Eain, V. Egan, J. Punch, P. Walsh, and E. Walsh, “An Investigation of the Pressure Drop Associated With Liquid-Liquid Slug Flows,” in ASME 2013 11th International Conference on Nanochannels, Microchannels, and Minichannels, Sapporo, Japan: American Society of Mechanical Engineers, Jun. 2013, p. V001T03A009. doi: 10.1115/ICNMM2013-73097.

[65] F. A. Hamad, F. Faraji, C. G. S. Santim, N. Basha, and Z. Ali, “Investigation of pressure drop in horizontal pipes with different diameters,” Int. J. Multiph. Flow, vol. 91, pp. 120–129, May 2017, doi: 10.1016/j.ijmultiphaseflow.2017.01.007.

[66] L. Amiri, S. A. Ghoreishi-Madiseh, F. P. Hassani, and A. P. Sasmito, “Estimating pressure drop and Ergun/Forchheimer parameters of flow through packed bed of spheres with large particle diameters,” Powder Technol., vol. 356, pp. 310–324, Nov. 2019, doi: 10.1016/j.powtec.2019.08.029.

[67] T. Yang et al., “Simple determination of key structural parameters for fibrous materials enabled by Ergun-Type and Kozeny-type equations,” Polym. Test., vol. 108, p. 107514, Apr. 2022, doi: 10.1016/j.polymertesting.2022.107514.

[68] https://www.justaskgemalto.com/fr/quest-ce-que-lintelligence-artificielle-et-lemachine- learning/

[69] « Machine d’Anticythère : Google célèbre l’ancêtre des calculateurs », lepoint.fr, 17 mai 2017, (www.lepoint.fr/ astronomie/machine-d-anticythere-google-celebre-l-ancetredes-calculateurs-17-05-2017-2127940_1925.php).

[70] http://www.fondapol.org/wp-content/uploads/2018/02/122-SOUDOPLATOF_2018-02-16_web.pdf (p14-p15) fév.2018

[71] https://www.quora.com/Does-the-brain-play-a-role-in-the-digestive-system

[72] QU'EST-CE QUE L'INTELLIGENCE ARTIFICIELLE ? Livret de vulgarisation Mission Villani sur l’intelligence artificielle Mars 2018

[73] http://villemin.gerard.free.fr/Wwwgvmm/Logique/IAintro.htm

[74] https://medium.com/@vjmanickam/weak-strong-ai-do-these-terms-matter-4bb57ce3a61f

[75] M. I. Jordan and T. M. Mitchell, “Machine learning: Trends, perspectives, and prospects,” Science, vol. 349, no. 6245, pp. 255–260, Jul. 2015, doi: 10.1126/science.aaa8415.

[76] K. R. Chowdhary, “Natural Language Processing,” in Fundamentals of Artificial Intelligence, New Delhi: Springer India, 2020, pp. 603–649. doi: 10.1007/978-81-322-3972-7_19.

[77] K. R. Chowdhary, Fundamentals of Artificial Intelligence. New Delhi: Springer India, 2020. doi: 10.1007/978-81-322-3972-7.

[78] H. Hassani, E. S. Silva, S. Unger, M. TajMazinani, and S. Mac Feely, "Artificial Intelligence (AI) or Intelligence Augmentation (IA): What Is the Future?," AI, vol. 1, no. 2, pp. 143–155, Apr. 2020, doi: 10.3390/ai1020008.

[79] https://www.techtarget.com/searchenterpriseai/tip/Types-of-AI-algorithms-and-how-they-work

[80] https://www.tableau.com/data-insights/ai/algorithms

[81] D. Ernst and A. Louette, "Introduction to reinforcement learning," 2024.

[82] B. Mahesh, "Machine learning algorithms-a review," Int. J. Sci. Res. IJSRInternet, vol. 9, no. 1, pp. 381–386, 2020.

[83] P. Cunningham, M. Cord, and S. J. Delany, "Supervised Learning," in Machine Learning Techniques for Multimedia, M. Cord and P. Cunningham, Eds., in Cognitive Technologies. , Berlin, Heidelberg: Springer Berlin Heidelberg, 2008, pp. 21–49. doi: 10.1007/978-3-540-75171-7_2.

[84] B. Charbuty and A. Abdulazeez, "Classification Based on Decision Tree Algorithm for Machine Learning," J. Appl. Sci. Technol. Trends, vol. 2, no. 01, pp. 20–28, Mar. 2021, doi: 10.38094/jastt20165.

[85] V. N. Vapnik, "An overview of statistical learning theory," IEEE Trans. Neural Netw., vol. 10, no. 5, pp. 988–999, Sep. 1999, doi: 10.1109/72.788640.

[86] V. Jakkula, "Tutorial on support vector machine (svm)," Sch. EECS Wash. State Univ., vol. 37, no. 2.5, p. 3, 2006.

[87] X.-Q. Bian, B. Han, Z.-M. Du, J.-N. Jaubert, and M.-J. Li, "Integrating support vector regression with genetic algorithm for CO2-oil minimum miscibility pressure (MMP) in pure and impure CO2 streams," Fuel, vol. 182, pp. 550–557, Oct. 2016, doi: 10.1016/j.fuel.2016.05.124.

[88] https://www.saedsayad.com/support_vector_machine_reg.htm

[89] A. G. Gad, "Particle Swarm Optimization Algorithm and Its Applications: A Systematic Review," Arch. Comput. Methods Eng., vol. 29, no. 5, pp. 2531–2561, Aug. 2022, doi: 10.1007/s11831-021-09694-4.

[90] D. Freitas, L. G. Lopes, and F. Morgado-Dias, "Particle swarm optimisation: a historical review up to the current developments," Entropy, vol. 22, no. 3, p. 362, 2020.

[91] R. Eberhart and J. Kennedy, "A new optimizer using particle swarm theory," in MHS'95. Proceedings of the Sixth International Symposium on Micro Machine and Human Science, Nagoya, Japan: IEEE, 1995, pp. 39–43. doi: 10.1109/MHS.1995.494215.

[92] J. Kennedy and R. Eberhart, "Particle swarm optimization," in Proceedings of ICNN'95 - International Conference on Neural Networks, Perth, WA, Australia: IEEE, 1995, pp. 1942–1948. doi: 10.1109/ICNN.1995.488968.

[93] L. Yi, "Study on an improved PSO algorithm and its application for solving function problem," Int J Smart Home, vol. 10, no. 3, pp. 51–62, 2016.

[94] E. H. Houssein, A. G. Gad, K. Hussain, and P. N. Suganthan, "Major Advances in Particle Swarm Optimization: Theory, Analysis, and Application," Swarm Evol. Comput., vol. 63, p. 100868, Jun. 2021, doi: 10.1016/j.swevo.2021.100868.

[95] Transpire Online, "A novel numerical optimization algorithm inspired from particles: particle swarm optimization," Transpire Online 2019, 2019.

[96] S. Mirjalili, "Dragonfly algorithm: a new meta-heuristic optimization technique for solving single-objective, discrete, and multi-objective problems," Neural Comput. Appl., vol. 27, no. 4, pp. 1053–1073, May 2016, doi: 10.1007/s00521-015-1920-1.

[97] T. Xie, J. Yao, and Z. Zhou, "DA-Based Parameter Optimization of Combined Kernel Support Vector Machine for Cancer Diagnosis," Processes, vol. 7, no. 5, p. 263, May 2019, doi: 10.3390/pr7050263.

[98] C. W. Reynolds, "Flocks, herds and schools: A distributed behavioral model," in Proceedings of the 14th annual conference on Computer graphics and interactive techniques, ACM, Aug. 1987, pp. 25–34. doi: 10.1145/37401.37406.

[99] X.-S. Yang, Nature-inspired metaheuristic algorithms. Luniver press, 2010.

[100] S. Mirjalili, S. M. Mirjalili, and A. Lewis, "Grey Wolf Optimizer," Adv. Eng. Softw., vol. 69, pp. 46–61, Mar. 2014, doi: 10.1016/j.advengsoft.2013.12.007.

[101] X.-Q. Bian, Q. Zhang, L. Zhang, and J. Chen, "A grey wolf optimizer-based support vector machine for the solubility of aromatic compounds in supercritical carbon dioxide," Chem. Eng. Res. Des., vol. 123, pp. 284–294, Jul. 2017, doi: 10.1016/j.cherd.2017.05.008.

[102] B. Üstün, W. Melssen, and L. Buydens, "Visualisation and interpretation of support vector regression models," Anal. Chim. Acta, vol. 595, no. 1–2, pp. 299–309, 2007.